

Sensor and Simulation Notes
Note 127
22 April 1971

PL/PA 16 DEC 96

Further Considerations for Multiturn Cylindrical Loops

Capt Carl E. Baum
Air Force Weapons Laboratory

Abstract

This note considers several aspects in the design of multi-turn loops including some techniques for improving the performance of such sensors. Multi-ax cable is used for the loop winding so as to distribute the signal input to several positions on the sensor structure. Combined with additional shorting conductors the multi-ax winding can be used to break up the first few resonances on the loop structure and so improve its high frequency performance. A finitely conducting shield can be placed around the loop to exclude the incident electric field at low frequencies and introduce some damping in resonances on the loop winding at higher frequencies. Highly conducting paths can be added to the shield surface to exclude unwanted magnetic field components. Such an anisotropic conducting shield routes current on the shield in preferential directions so as to re-distribute unwanted currents along paths with negligible coupling to the loop. Tabulation is made of the loop inductance for an idealized uniform surface current density around a finite length cylinder and some corrections to this inductance for the size and spacing of the turn conductors are considered.

Sensor and Simulation Notes
Note 127
22 April 1971

Further Considerations for Multiturn Cylindrical Loops

Capt Carl E. Baum
Air Force Weapons Laboratory

Abstract

This note considers several aspects in the design of multi-turn loops including some techniques for improving the performance of such sensors. Multiax cable is used for the loop winding so as to distribute the signal input to several positions on the sensor structure. Combined with additional shorting conductors the multiax winding can be used to break up the first few resonances on the loop structure and so improve its high frequency performance. A finitely conducting shield can be placed around the loop to exclude the incident electric field at low frequencies and introduce some damping in resonances on the loop winding at higher frequencies. Highly conducting paths can be added to the shield surface to exclude unwanted magnetic field components. Such an anisotropic conducting shield routes current on the shield in preferential directions so as to redistribute unwanted currents along paths with negligible coupling to the loop. Tabulation is made of the loop inductance for an idealized uniform surface current density around a finite length cylinder and some corrections to this inductance for the size and spacing of the turn conductors are considered.

I. Introduction

In designing loops sensitive to the time rate of change of the magnetic field one may wish to have a large equivalent area to give the sensor a large sensitivity. For limited maximum sensor dimensions one may use many loop turns to achieve some large loop area. In so doing the inductance of the sensor increases as the square of the number of turns (for a fixed sensor size). If the load driven by the loop is some fixed resistance (as in the case of the characteristic impedance of a signal cable) then the upper frequency response of the loop (in terms of the time derivative of the magnetic field) decreases as N^{-2} where N is the number of loop turns. For frequencies above this inductive-resistive limitation the sensor output into such a frequency independent resistive load is proportional to the magnetic field. However, this applies only up to frequencies for which the loop begins to be no longer electrically small or for which various resonant effects on the many loop turns begin to influence the response of the sensor. With a multiturn loop such resonances can occur if the entire length of the loop turns (a total of N turns laid out in a line) is roughly of the order of the wavelength or an appropriate factor times the wavelength depending on the specifics of the loop design. While one may be designing a sensor as a low frequency sensor for $\partial B/\partial t$, still one could advantageously use its response to B at higher frequencies in the sense of a known well-behaved transfer function. This response to B will hold only up to some high-frequency limit related to loop size, turn configuration, and other characteristics of the loop geometry. In designing a multiturn loop one might like to make the high-frequency response to B extend out to as high a frequency as possible, besides making the upper frequency response to $\partial B/\partial t$ for a given sensitivity and sensor size extend to as high a frequency as possible.

Previous notes have dealt with some aspects of the design of multiturn loops, including geometric arrangement of the turns, inductance, sensor shape, and resistive shields for reducing the electric field in the vicinity of the loop turns. In this note we further develop some of these considerations and also add some new ones. First we apply some techniques using multi-ax cable for the turns to distribute the signal input positions around the multiturn structure and thereby improve high frequency performance. Second we consider adding highly conducting metal current paths on resistive shields in directions which do not significantly perturb the magnetic field component being measured by the sensor. Third we consider some of the electrical connections between the loop conductors and a surrounding resistive shield. Finally we give some further consideration to the loop inductance for uniform turn spacing on a circular cylinder. While our illustrations and examples are for circular cylindrical loops for measuring the component of $\partial B/\partial t$ parallel to the loop axis, the general considerations involving use

of multi-ax cable, appropriate conductors with resistive shields, and electrical connections between resistive shields and loop turns apply to various other loop geometries such as spheres, spheroids, rectangular parallelepipeds, and circular cylinders (for the additional case of measuring a component of the magnetic field perpendicular to the cylinder axis).

II. Multi-ax Cable Used as the Winding for a Multiturn Loop and for Distributing the Signal Input Positions

In a previous note¹ we have discussed the use of multi-ax cable for distributing the signal input going to a single position such as to a cable which transports the analog signal from the sensor. This was discussed from the viewpoint of single turn loops for the most part. This technique allows one to take signals from evenly spaced positions around the loop with effectively identical impedances introduced at each such position; the signals from the n signal introduction positions propagate inside the multi-ax cable and combine with equal delays from the signal introduction positions at various positions inside the multi-ax cable. For a single turn loop this technique can be used to improve the high frequency performance by decreasing the effective capacitance associated with the loop gaps and eliminating the peaks (resonances) from the loop response so that the high frequency performance is only limited by transit times across the loop diameter; also the undesirable dependence of the high frequency response on the direction of wave incidence is significantly reduced. In this previous note various other examples were at least briefly mentioned which included fractional turn loops and the use of moebius loop gaps together with multi-ax cable for the loop conductors. For n signal introduction positions there was also considered an N turn loop for the special case that $N = n$. For this special case the multiturn loop can be made as a conducting finite length cylinder with a full length slot with the multi-ax cable crossing the slot at each of the signal introduction positions. With the outermost shield slotted cylinder the sensor behaves as a slotted cylinder with n equal resistive impedances loading the slot; for its high-frequency performance it behaves as a one turn cylindrical loop irrespective of whether $N (= n)$ is 2, 4, 8, etc.

In this note we consider the case that the number of loop turns N is not the same as the number of signal introduction positions n . Generally if N is made very large so as to obtain a corresponding large equivalent area for the loop then $N \gg n$ since n is limited by

1. Lt Carl E. Baum, Sensor and Simulation Note 23, A Technique for the Distribution of Signal Inputs to Loops, July 1966.

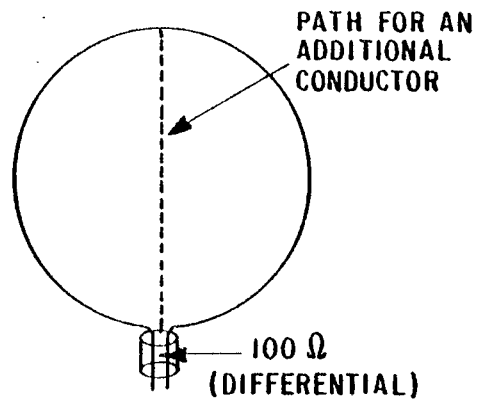
$$n = 2^{M-1} \quad (1)$$

for a single coax output from the multi-ax where M is the number of transmission lines in the multi-ax. If differential (twin-ax) output is used to combine outputs from both ends of a multi-ax then

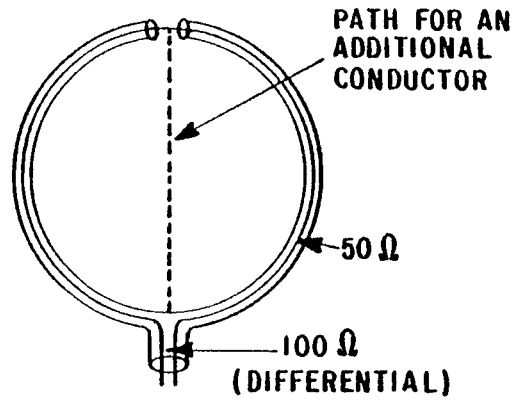
$$n = 2^M \quad (2)$$

In either case M is practically limited to small integers (1 (coax), 2 (triax), and perhaps a few higher orders) because of mechanical limitations associated with the small impedances for the outermost transmission lines; this then also practically limits the size of n. For a sensitive multiturn loop one may want 10, 20, 50, 100, etc. for N, the number of turns. However, multi-ax can be used as the basic item to construct the N turns of the loop. Even if the loop still behaves as an N turn loop in its interaction with an incident field distribution high frequency resonances associated with the full length of the N turns can be damped by the distribution of the load impedance to the n signal introduction positions approximately uniformly spaced (which is consistent with equalizing internal transit times in the multi-ax) along the extended length of the full N turns. Furthermore additional conductors can be connected to the loop turns midway between the signal introduction positions to reduce the total turn length into smaller turn groups with the first resonance for the current on the exterior of the multi-ax (forming the loop turns) at a somewhat higher frequency.

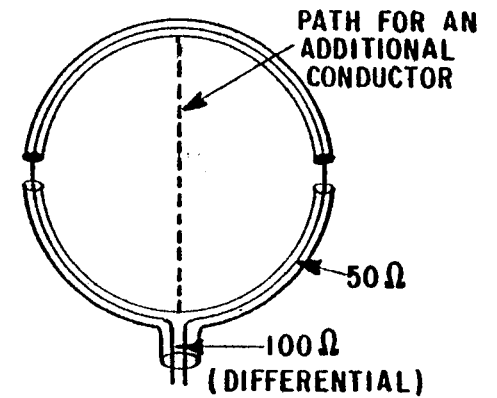
As a first step in considering the use of multi-ax cable for multiturn loops begin with the single turn differential loop geometries shown in figure 1. Here the entire multiturn structure is stretched out as one large single turn for illustration. The complete loop is made of two symmetrical halves with each half driving one of the leads of a differential signal output, say twin-ax. Alternatively the output might be two coax cables with shields bonded together, or might be some kind of telemetry unit. Note that if only one side of the loop structure from any case in figure 1 is used, a single ended loop (with only half the number of signal introduction positions) can be made by connecting the end of the multi-ax cable away from the coax output back to the coax output position. In the examples in figure 1 the coax output would be at the bottom and the other end of the multi-ax cable would be at the top; to form the single ended loop take either the left or right half and join the ends by contracting the vertical line labeled as a path for an additional conductor. The impedances chosen for the examples in figure 1 are based on a 100 Ω differential output; the important feature of the impedances is that starting



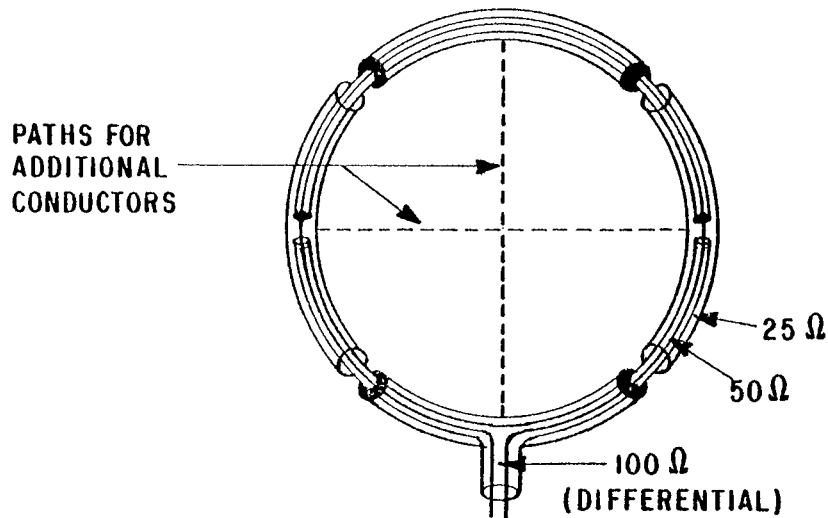
A. WIRE OR STRIP WITH SINGLE LOOP "GAP"



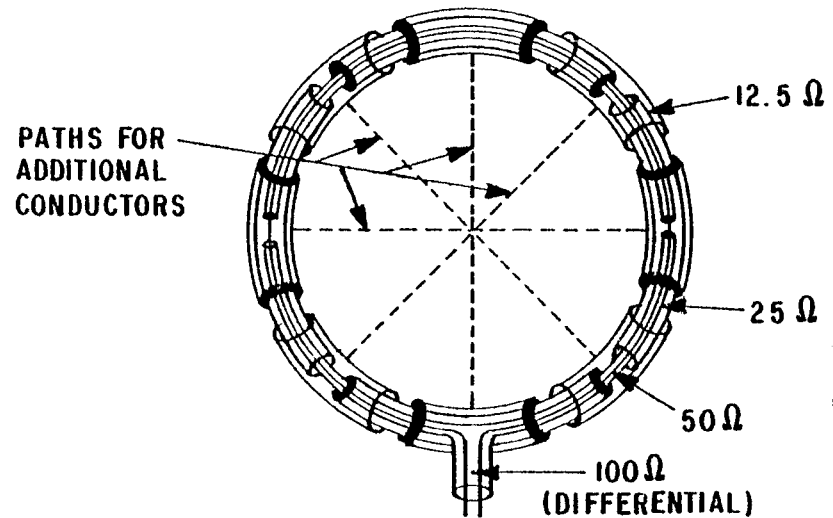
B. COAX WITH SINGLE LOOP GAP



C. COAX WITH TWO LOOP GAPS



D. TRIAX WITH FOUR LOOP GAPS



E. QUADRAX WITH EIGHT LOOP GAPS

FIGURE 1. TYPES OF MULTIAX WINDINGS FOR MULTITURN LOOPS WITH DIFFERENTIAL OUTPUTS UNWOUND IN THE FORM OF SINGLE TURN LOOPS

from the center of the multi-ax the impedance between successive coaxial conductors is cut in half in each successive outward step. The coax which starts the multi-ax is 50Ω for these examples, but could be some other convenient impedance such as 100Ω .²

Figure 1 shows a progression of loop geometries (single turn) up through some of the structures involving multi-ax which have a larger number of signal introduction positions n around the loop structure. Beginning in figure 1A we have a single turn of wire driving a differential output. For lower inductance this wire might be made into a strip; when wound into a multiturn cylindrical loop we have various winding geometries considered for this case in a previous note.³ This kind of loop can have a large electric field response in the common mode and so an additional conductor can be advantageously used to short out the common mode with an inductive impedance much smaller in magnitude than the output cable impedances (common and differential modes) for most of the frequencies of interest. This "center point grounding" technique is also useful for shorting out common mode signals associated with high energy electrons produced by a nuclear radiation environment; in this respect "center point grounding" gives advantages similar to a Moebius loop gap which shorts out such a radiation induced common mode but which also doubles the number of loop turns.⁴ In this note we are not concerned primarily with measurements in nuclear radiation environments, so the "center point grounding" for this case would be for reduction of the electric field induced common mode.

Instead of a single turn of wire one might make a loop from a coaxial cable with a loop gap at the opposite extremity from the differential output as shown in figure 1B. The extension of coaxial shields from the differential output shield can be used to greatly reduce the electric field induced common mode currents which can be present in the configuration of figure 1A (without "center point grounding"); the common mode current is made to flow on the shield instead of the center conductor of the coax. There can still be some much smaller common mode pickup associated with the coupling of the electric field to the center conductor in the loop gap itself. As shown in figure 1B one can also place an additional conductor along a symmetry plane of the loop without affecting the differential signal. This gives a "center point ground" to provide an inductive

2. All units are rationalized MKSA.

3. Capt Carl E. Baum, Sensor and Simulation Note 43, Some Considerations for Electrically-Small Multi-Turn Cylindrical Loops, May 1967.

4. Lt Carl E. Baum, Sensor and Simulation Note 7, Characteristics of the Moebius Strip Loop, December 1964.

short for common mode signals to short out to the shield at the signal output position on the loop structure. Of course since some common mode signal (more than in the loop gap) is induced on this additional conductor then the extra conductor may not be useful unless frequencies of interest are low enough that the inductive common mode short reduces the common mode signal more than the electric field pickup of this conductor increases the common mode signal. These considerations have been related to reducing electric field induced common mode signals. If one considers nuclear radiation induced common mode signals then the "center point grounding" technique is quite important and achieves the same kind of result (except with only a single turn) as a loop with the moebius gap (ref. 4); the loop design in figure 1B uses what can be termed a split shield gap. For our present considerations nuclear radiation interaction is assumed not significant so "center point grounding" via the additional conductor is not necessarily desirable.

A next improvement involves using two loop gaps as is the case in the example using coax in figure 1C. The two loop gaps are at opposite positions around the loop winding and symmetrically located with respect to the output position giving equal signal delays from the loop gaps to the differential output. Just as in the previous two cases (figures 1A and 1B) an additional conductor can be symmetrically positioned on the loop to connect the signal conductor at its center to the signal shield near the signal output position. This additional conductor provides an inductive short for the electric field associated common mode signal produced on the part of the loop away from the signal output (beyond the two loop gaps). This conductor also greatly reduces nuclear radiation induced common mode signals. In going to two loop gaps instead of one the high frequency performance of the loop as a sensor is improved in two ways. The capacitance of the loop gaps is decreased by placing more than one effectively in series. The uniformly spaced loop gaps with identical time delays and impedances make the output signal sum the signals from around the loop structure thereby removing some of the higher order current modes on the loop structure from any contribution to the output signal; this reduces the unwanted dependence of the output signal on the direction of wave incidence relative to the loop. This improvement in the high frequency performance for single turn toroidal loops through the use of multiple loop gaps is similar to that for cylindrical loops which has been considered in some detail in a previous note.⁵

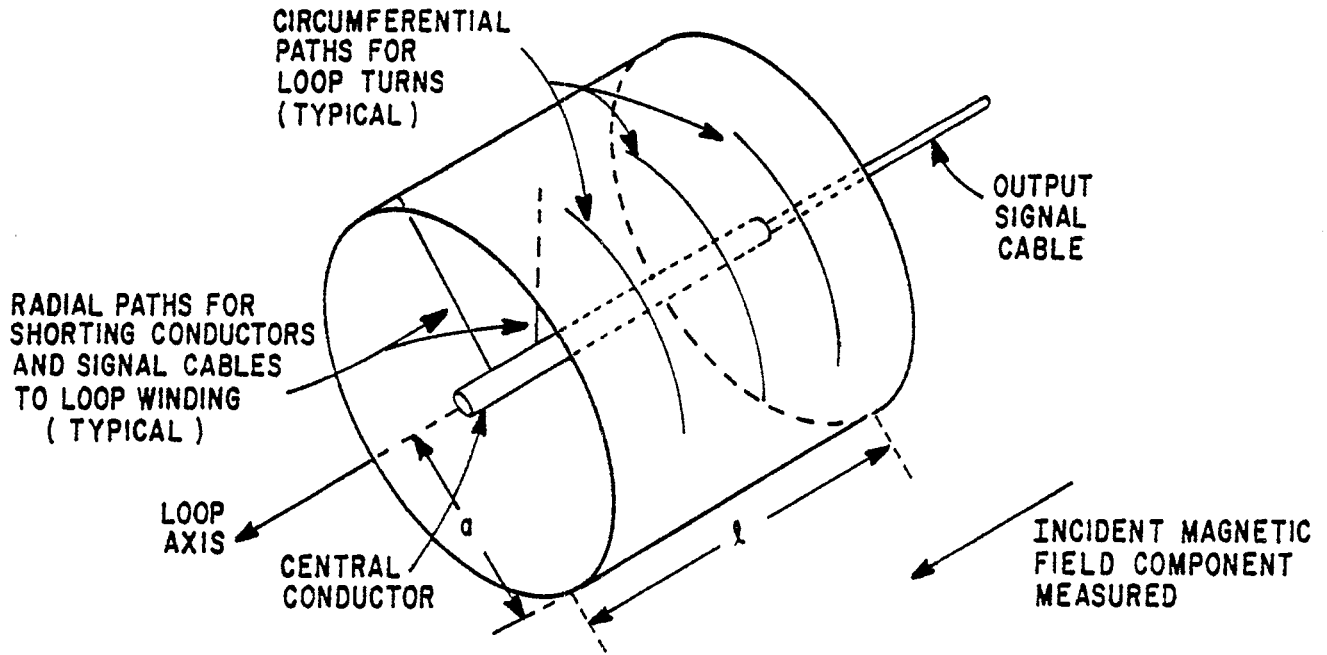
Going on to figure 1D triax can be used to give $n = 4$ signal input positions uniformly spaced around the loop structure. As indicated in this figure additional conductors can run from

5. Capt Carl E. Baum, Sensor and Simulation Note 41, The Multi-Gap Cylindrical Loop in Non-Conducting Media, May 1967.

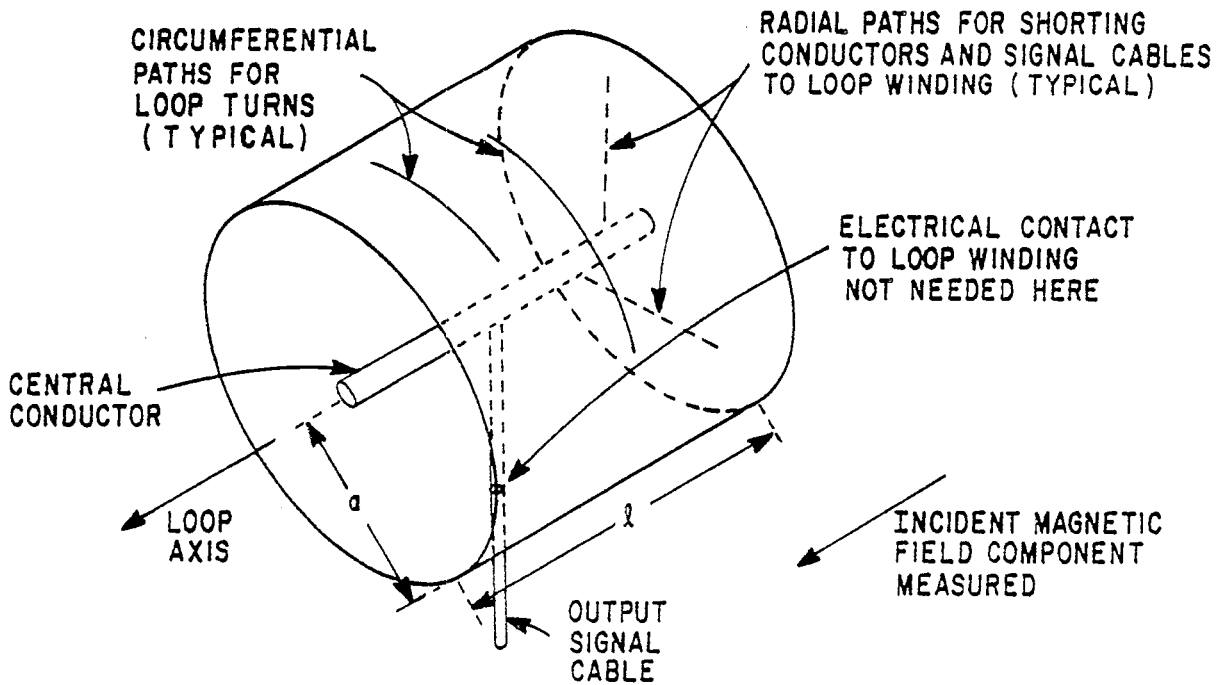
the center of the loop to four positions on the loop structure centered between the loop gaps. Besides shorting out the electric field associated common mode signal with an inductive short some higher order current modes on the loop structure are also reduced by the additional inductive shorts, although these are less important, except perhaps for providing a low frequency short to the otherwise floating sections of the outer triax shield.

Figure 1E shows quadrax being used to make a loop with $n = 8$ signal input positions uniformly spaced around the loop. In this case shorting conductors can be connected to eight positions on the loop structure from the loop center. With $n = 8$ even better high frequency characteristics can be obtained. These examples can be extended to arbitrarily large order M of the multi-ax cable as outlined in reference 1, limited only by the practical impedances attainable between successive shields.

Having considered the basic multi-ax structure for the loop winding let us now consider the geometry of the multiturn cylindrical loop structure and positioning of the multiturn windings with the n signal introduction positions and appropriate additional shorting conductors. To begin consider three basic parts of the loop structure shown in figure 2. First there is the circular cylindrical surface defining the position of the multi-ax winding. Since we are only considering the case of measuring the magnetic field component parallel to the cylinder axis then the loop turns are wound perpendicular to this axis on the cylindrical surface except for the interconnection from turn to turn or the effective pitch of a "helical" winding. Second there is a conductor along the central axis of the cylinder. This conductor forms a common electrical tie for the sensor. From this conductor shorting conductors can be connected out to the winding on the winding surface mentioned above; such connections are made to positions on the multi-ax winding at positions between the signal input gaps corresponding to the examples shown in figure 1 (with the winding shown as a single turn). Third the output signal cable may come into the central conductor in one of two symmetrical fashions. It can come in along the loop axis (giving what is called an axial model) and form a direct extension of the central conductor. Alternatively it can come into the central conductor at right angles (giving what is called a radial model), positioned midway between the two ends of the truncated cylinder defining the maximum extent of the windings as well as the central conductor. If some kind of telemetry is used to transmit the signal from the sensor without using an output cable the telemetry unit (modulator, transmitter, power supply) might be packaged as part of this central conductor. Note, however, for convenience in accurately calculating the equivalent area of the loop the central conductor as well as other conductors should present minimum distortion to the incident magnetic field component being measured. Signals are taken from the winding on the cylindrical surface to the central



A. AXIAL SIGNAL OUTPUT CONFIGURATION



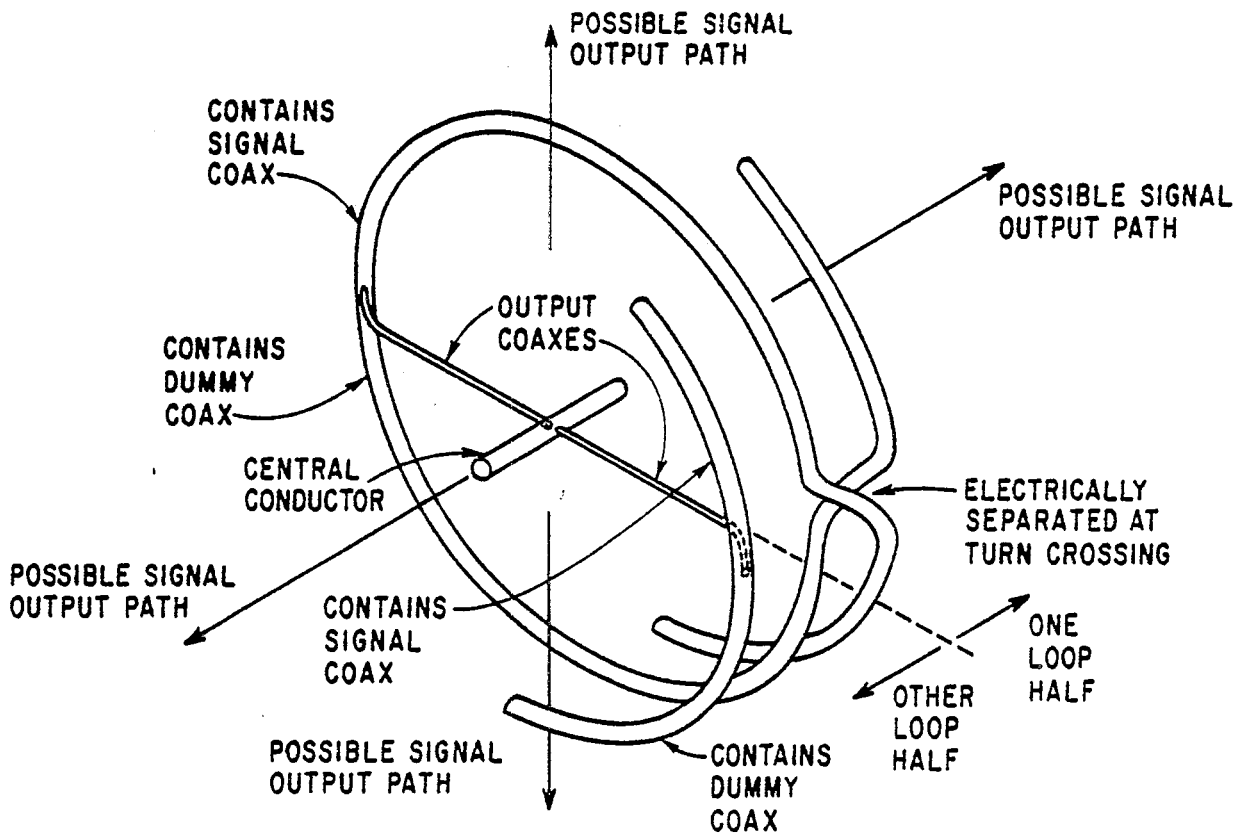
B. RADIAL SIGNAL OUTPUT CONFIGURATION

FIGURE 2. GEOMETRY OF LOOP STRUCTURE

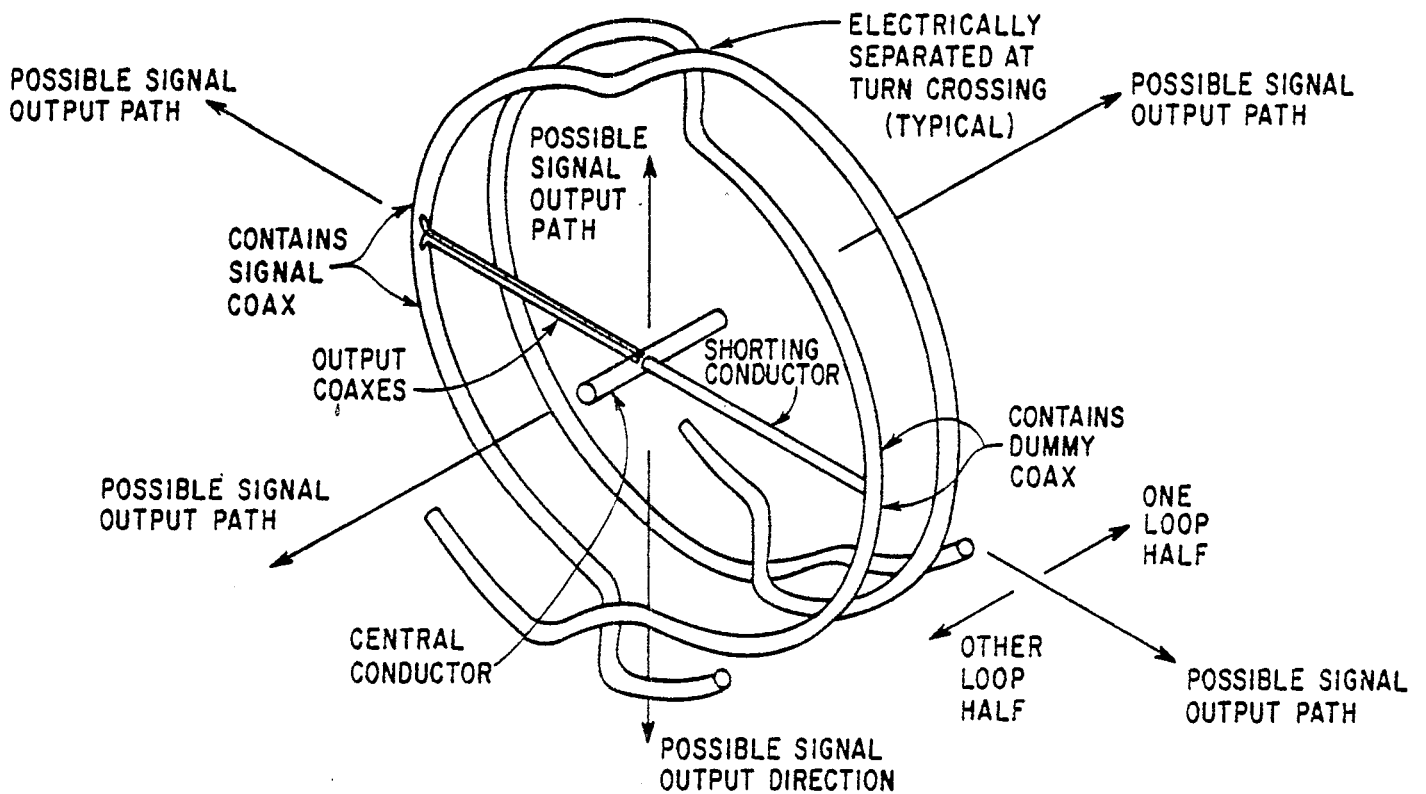
conductor via signal cables (coax or twinax) with their shields being used as shorting conductors from the multi-ax winding to the central conductor thereby serving the same kind of function as the added shorting conductors mentioned above.

With the overall geometry of this type of multiturn loop design specified let us go into a little more detail. From figure 1 we have the overall multi-ax winding with n signal input positions and n shorting positions with $n = 1, 2, 4, 8, \dots$ for a differential loop output. This full winding can be divided into two symmetrical halves (left and right in each part of figure 1). For our multiturn loop then let us consider each half of the winding. If the number of loop turns N is even so that $N/2$ is an integer then we can have the geometry of a half winding as shown in figure 3A. Note that the half winding has only one coaxial signal exit; the inner coax at the other end of the half winding is not being used to carry a signal inside it and is effectively a dummy. This half winding starts at some position near the circle dividing the cylindrical winding surface into two equal finite length circular cylinders, winds $N/4$ turns in reaching the end of the cylindrical winding surface, and winds $N/4$ turns in returning to the starting position where the multi-ax shields connect together to form the loop. The coax for the signal output is then extended radially to the central conductor of the loop structure where it is joined with the signal from the second half winding to give the differential output. Each half winding (and thus the total loop) is wound in counterwound fashion as discussed in a previous note (ref. 3) except that multi-ax windings are used instead of strips or wires. The coaxial output from each loop half can be considered in addition as one of the shorting conductors from the winding to the central conductor. As shown in figure 3A the coaxial outputs from the two loop halves leave the central conductor in opposite radial directions which are on the same straight line and perpendicular to both axial and radial directions for the signal output cable. Other designs for N even are possible with other kinds of symmetry such as that obtained by making the two coaxes for the loop halves leave the central conductor in the same radial direction as one shorting conductor.

For N odd each loop half has a non integer number of turns. One might make a half turn at the output of each loop half in combination with the coax output from each loop half by a design such as that shown in figure 3B. Here the two coaxes from the two loop halves go as one shorting conductor to the central conductor and a shorting conductor is symmetrically extended to the loop winding. Designs which have the two output coaxes in opposite radial directions are also possible. The remaining half turn for each loop half can also be taken care of at the two ends of the finite cylindrical loop surface where the centers of the windings for each loop half are located by having the winding leave the cylindrical winding surface to pass



A. N EVEN WITH 2 OUTPUT COAXES IN OPPOSITE DIRECTIONS FROM CENTER



B. N ODD WITH 2 OUTPUT COAXES IN SAME DIRECTION FROM CENTER

FIGURE 3. SIGNAL OUTPUT CONNECTIONS FROM WINDING FOR EACH HALF LOOP NEAR THE LOOP CENTER

through the cylinder axis (connecting to the central conductor if $n = 4, 8, \text{etc.}$) and go back to the winding surface on the opposite side.

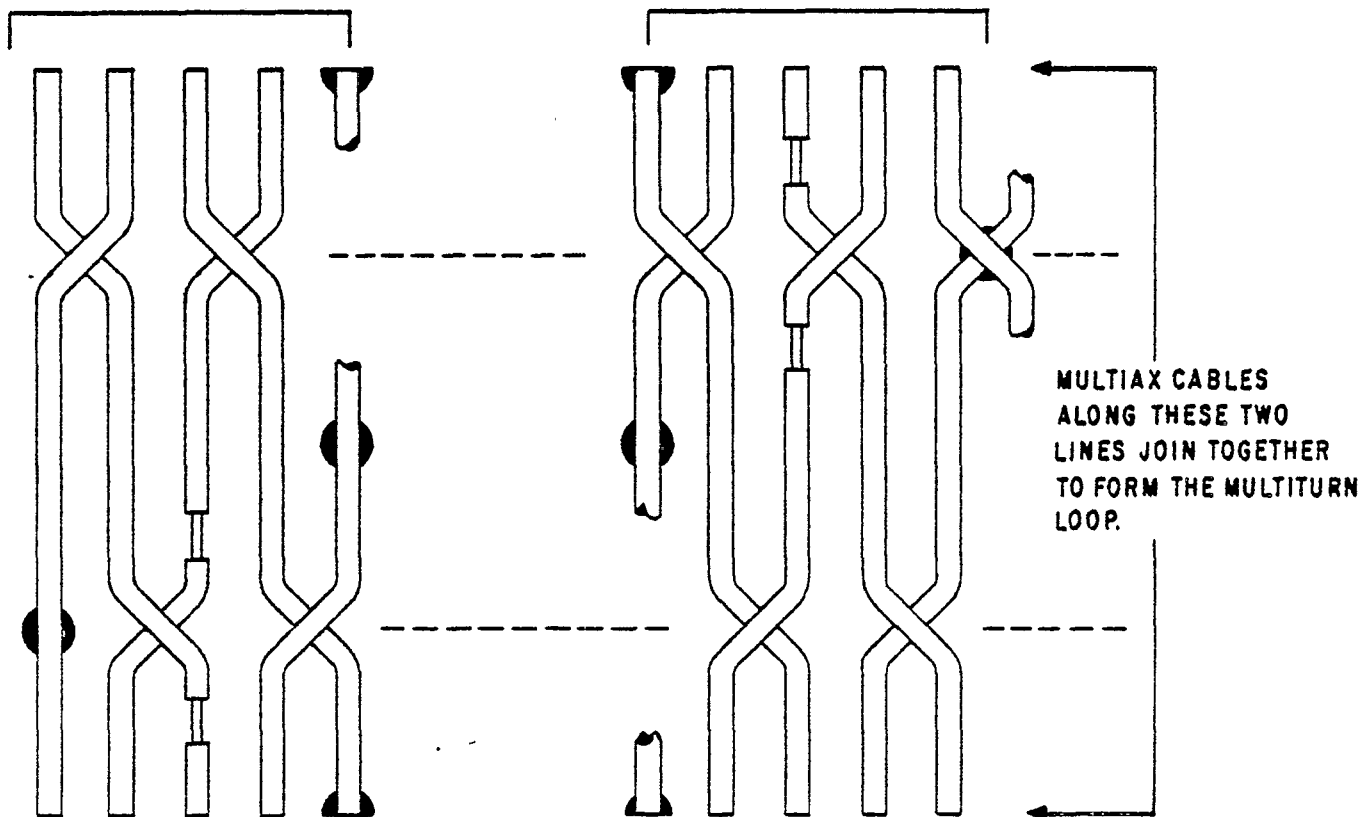
Now consider some features of the multi-ax winding. This winding has n signal introduction positions evenly spaced along the total winding and centered along the winding between positions for shorting conductors which may connect the winding to the central conductor on the loop axis. For convenience we define each part of the winding (on the cylindrical winding surface) going between two such shorting positions as a turn group. The total loop then has n turn groups and N/n turns per turn group. There is a signal introduction position at the midpoint of the winding for that turn group.

In a previous note (ref. 3) we have considered some features of a counterwound loop winding. In using this technique with a multi-ax winding with differential output each loop half winds from the center to one end and back to the center. For $n = 2$ each loop half is one turn group. For $n = 4, 8, \dots$ the turn groups are positioned in pairs in their location on the cylindrical winding surface with the two groups in the pair being counterwound through one another over the same linear extent along the loop axis. Depending on whether the number of turns N/n in a turn group is an integer, a half integer, etc. the shorting positions and signal introduction positions of the two paired counterwound turn groups may occur at the same position by pairs on the cylindrical winding surface, on opposite sides of this surface with respect to the loop axis, or some other angular relation with respect to the loop axis. It depends on the number of turns $N/(2n)$ between a shorting conductor and a signal introduction position and which turn group one is considering as one moves parallel to the loop axis along the cylindrical winding surface.

Figure 4 shows four turn groups (two pairs) selected from a counterwound multi-ax winding which is chosen to have $N/n = 2.25$ turns per turn group. The first pair is taken at the end of the loop and it is assumed that the loop winding only makes full turns here (stays on the winding surface). The second pair is chosen somewhere along the winding surface away from both ends of a loop half (away from both ends and center of the loop). Note the alternation in the way the turns cross over one another (at opposite sides of the winding surface with respect to the loop axis). This is for averaging out the increase and decrease of the loop equivalent area associated with the departure of the winding from the cylindrical winding surface, thereby making an accurate calculation of the equivalent area more convenient. The scheme shown in figure 4 can be thought of as a repetitive application of a sequence over-under-under-over in any turn group with the paired turn group in the counter winding having the over and under reversed at each turn crossing. The turns make no conducting electrical contact at these turn

TURN GROUP PAIR AT ONE
END OF THE LOOP

TURN GROUP PAIR SOMEWHERE
ALONG THE LOOP STRUCTURE



● AND  INDICATE POSITIONS WHERE SHORTING CONDUCTORS LEAD FROM THE MULTIAX WINDING(S) TO THE CENTRAL CONDUCTOR (NOT SHOWN).

 INDICATES A SIGNAL INTRODUCTION POSITION INTO THE MULTIAX CABLE.

FIGURE 4. EXAMPLE OF PAIRS OF COUNTER WOUND MULTIAX TURN GROUPS: EXPANDED VIEW FOR $N/n = 2.25$

crossings unless the crossing position also happens to be an electrical shorting position for both of the crossing conductors. In figure 4 the winding has been cut parallel to the loop axis and laid out for illustration. Figure 3 shows a few turn crossings in an angular view of portions of loop windings. By alternating the over and under crossings of the windings (such as by the scheme discussed) one can also try to minimize coupling to other field components associated with these perturbations in the ideal cylindrical windings.

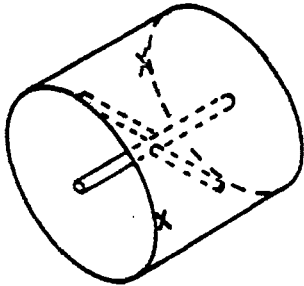
Having defined turn groups and turn group pairs one can electrically connect electrically similar positions within the turn group pairs and from one pair to other pairs via conducting paths which do not interfere with the magnetic flux parallel to the loop axis. These conductors would basically run parallel to the loop axis as does the central conductor but on neither the loop axis nor the winding surface; radial conductors would then connect the appropriate winding positions to the axial conductors. Alternatively these paths might not be made of highly conducting metal but might be partly or entirely made of some resistive material to provide some damping for unwanted resonances at high frequencies on the loop structure. For convenience these are not shown in figure 4 or in other figures; the possible variations in such extra links between loop turns are quite large in number. Note that the turns in figure 4 are evenly spaced along the loop axis. This is not necessary and one might use a variable spacing to try to reduce the loop inductance for a given N and loop dimensions. Including the turn crossings, a variable turn spacing gives a slight variation in the winding lengths for each turn group and/or slightly shifts the positions of the shorting conductors and the signal input positions around the winding surface. Alternatively the variation could be made up by allowing a variable extra length of winding in each turn, still keeping the winding on the winding surface except right at the turn crossing positions.

Having looked at some details of the windings let us next see how some features of the turn groups might fit into the total loop geometry. For this purpose consider some examples for $n = 2$ and $n = 4$ signal introduction positions and the same number of shorting positions. For these examples let the total number of loop turns N be even and let the two loop halves with $N/2$ turns each be joined in the center of the loop in the manner shown in figure 3A. For each choice of n one must choose the even integer N such that $N/(2n)$ gives a particular remainder after subtraction of the integer part. We might then choose $N/(2n) = \text{integer}$, $\text{integer} + 1/2$, $\text{integer} + 1/4$, etc. The factor $2n$ is used because this is the sum of the number of positions of both signal introduction (indicated by x) and shorting (shown by a conductor from the central conductor). Figure 5A takes the case of $n = 2$ with only two shorting conductors (two coax outputs from the two loop halves). Here there are 2 cases corresponding to $N/(2n) = \text{integer}$ and $N/(2n) = \text{integer} + 1/2$

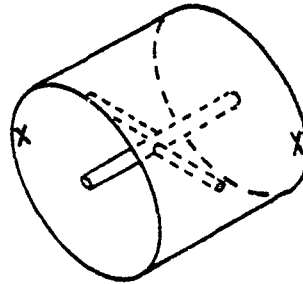
□ INDICATES THE CENTRAL CONDUCTOR, OUTPUT COAXES FROM THE LOOP HALVES, AND SHORTING CONDUCTORS.

X INDICATES A SIGNAL INTRODUCTION POSITION ON THE MULTIAX WINDING.

* INDICATES TWO MULTIAX SIGNAL INTRODUCTIONS AT THE SAME POSITION ON THE WINDING SURFACE.

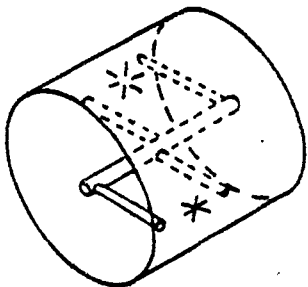


$$\frac{N}{2n} = \text{INTEGER}$$

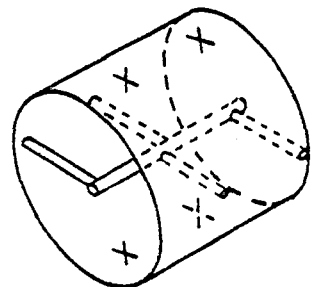


$$\frac{N}{2n} = \text{INTEGER} + 1/2$$

A. $n = 2$ SIGNAL INTRODUCTION POSITIONS

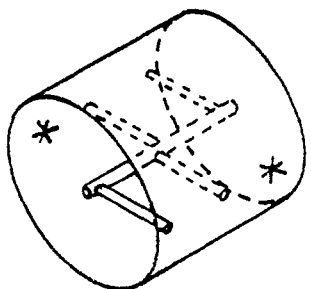


$$\frac{N}{2n} = \text{INTEGER}$$

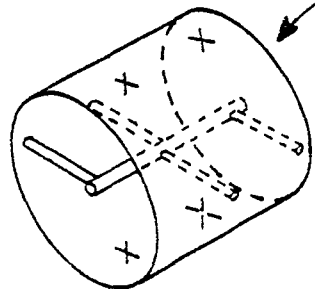


$$\frac{N}{2n} = \text{INTEGER} + 1/4$$

THESE TWO CASES LOOK THE SAME BECAUSE THE SIGNAL INPUT POSITIONS ON OPPOSITE SIDES OF THE CYLINDER HAVE SWITCHED PLACES.



$$\frac{N}{2n} = \text{INTEGER} + 1/2$$



$$\frac{N}{2n} = \text{INTEGER} + 3/4$$

B. $n = 4$ SIGNAL INTRODUCTION POSITIONS

FIGURE 5. GEOMETRY OF SHORTING POSITIONS AND SIGNAL INTRODUCTION POSITIONS FOR N EVEN WITH OUTPUT COAXES FROM LOOP HALVES IN OPPOSITE DIRECTIONS FROM CENTER

which give different positions for the two signal introduction positions. Figure 5B takes the case of $n = 4$ with shorting conductors at the center and at the ends of the cylindrical loop structure while the signal introduction positions are midway between the center and the two ends. For $n = 4$ there are 4 cases corresponding to $N/(2n) = \text{integer}$, $\text{integer} + 1/4$, $\text{integer} + 1/2$, and $\text{integer} + 3/4$. Note that figure 5 is somewhat schematic in that the actual windings are not shown; these results apply to many different numbers of turns. Also note in figure 5B that the cases of $\text{integer} + 1/4$ and $\text{integer} + 3/4$ give the same pattern of shorting and signal introduction positions and so might be considered as the same basic type of multiturn loop design. This same pattern results because increasing N by 4 turns increases the winding in one turn group (one half the winding of one loop half) by 1 turn, thereby shifting the signal introduction position in that turn group by $1/2$ turn placing it on the opposite side of the cylindrical winding surface; this signal introduction position has then switched places with the one in the other turn group in the same turn group pair forming the half loop.

Figure 5 diagrammatically shows the kinds of symmetries one can obtain for the shorting positions and signal input positions for multiturn loops using a certain type of multi-ax winding. This can be extended to $n = 8, 16, 32$, etc. in a straightforward manner. As n increases the number of possible patterns or geometries for the shorting positions and signal input positions becomes quite large. Furthermore we have just been considering the examples for n even formed by having the output coaxes from the two loop halves in opposite radial directions with respect to the central conductor. One can also set up this kind of shorting and signal input diagram for the case of the output coaxes in the same direction, or one can have N odd as in figure 3B with the output coaxes together, or for N odd one can place the output coaxes in opposite directions. One can also use fractional turns by routing the multi-ax winding from the winding surface to the central conductor and back again at the loop ends or even at the ends (shorting positions) of any of the turn groups. However, one may wish to keep the multi-ax winding length the same for each turn group with the signal introduction position in the center of the turn group winding to equalize transit times from all signal introduction positions to the loop output, although some variations are possible even here. In summary, for multiturn loops using multi-ax windings the number of design variations is enormous.

Having considered the geometry of the shorting positions and signal input positions let us briefly consider some of the qualitative design benefits associated with multi-ax windings with shorting positions midway between successive signal input positions. Near the beginning of this section when discussing the multi-ax configuration as in figure 1 to be used for making the multiturn winding an important feature was pointed out.

Specifically with equally spaced signal input positions then a circular loop has a current on it which can be expressed as a Fourier series in the angular variable around the loop. With n identical signal input positions equally spaced around the loop then the zero order (uniform current) term and the n th term contribute to the net signal output but all the terms in between are cancelled out. This effect is considered in detail for infinitely long cylindrical loops in ref. 5. It is the zero order term in the current which is uniform around the loop that one is interested in for a magnetic field measurement. The higher order terms correspond to other features of the electromagnetic field distribution. Furthermore resonances are also associated with some of these higher order terms, thereby making the frequency response characteristics of the loop non ideal at high frequencies instead of simply proportional to the magnetic field or its time derivative. The high frequencies where these resonance effects first set in are those for which the wavelength is of the order of the loop circumference.

Now apply these considerations to multiturn loops. As a very rough approximation look at the multiturn winding as a transmission line with length the same as the winding length d and propagation velocity about the same as the medium in which it is placed (typically free space for many applications). The impedance of this transmission line would be related to the diameter of the winding (outer multi-ax shield), the spacing to some of the nearby turns in the winding, and the wave impedance of the medium around the winding. However the impedance does not concern us here. This winding in the form of a multiturn cylindrical loop is placed in some electromagnetic field distribution which excites a current in the winding. One can expand this current in a Fourier series with terms of the form $\cos(2n_1\pi\zeta/d)$ and $\sin(2n_1\pi\zeta/d)$ where ζ is a conveniently defined distance along the winding from some arbitrary starting position and $n_1 = 0, 1, 2, 3, \dots$. If the signal input positions are shorted out giving zero impedance in series with the transmission line (model of the winding) then these sinusoidal terms can be roughly thought of as eigenmodes of the winding. These are schematically indicated up through $n_1 = 4$ in figure 6A with the loop winding laid out as a circle.

A point of interest is that while the cylindrical loop winding surface of length l and radius a may have both l and $2a$ small compared to a wavelength at some moderately high frequency of interest, the winding of length d may have its length comparable to a wavelength. Note that the winding length is approximately

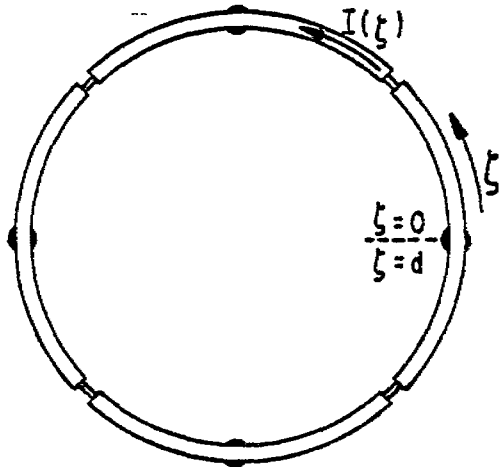
$$d \approx 2\pi a N \quad (3)$$

|| AND ● INDICATE SHORTING POSITIONS (INCLUDING COAX OUTPUT).

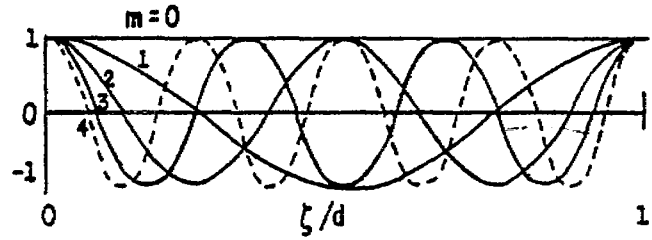
U AND X INDICATE SIGNAL INTRODUCTION POSITIONS.

SIGNAL INPUT AND SHORTING POSITIONS

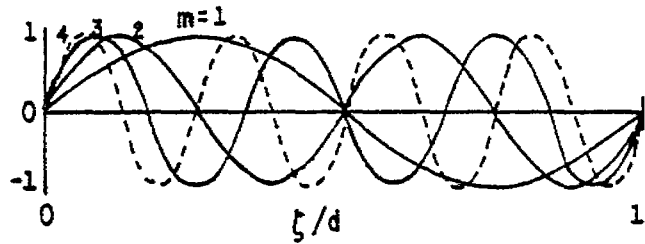
● X ● X ● X ● X ●



EXTENDED LOOP WINDING



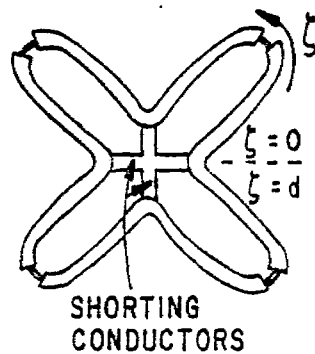
$\cos(2n_1\pi\xi/d)$ TERMS



$\sin(2n_1\pi\xi/d)$ TERMS

FIRST SEVERAL TERMS IN FOURIER EXPANSION OF CURRENT ON WINDING

A. LOOP WINDING EXTENDED WITH SHORTING CONDUCTORS ABSENT



SHORTING CONDUCTORS

B. LOOP WINDING EXTENDED OUT WITH SHORTING CONDUCTORS OF SMALL LENGTH INCLUDED

FIGURE 6. APPROXIMATE CURRENT DISTRIBUTION AND HIGH FREQUENCY RESONANCES ON MULTITURN LOOP WINDINGS: EXAMPLE WITH $n = 4$

if the extra length associated with the turn crossings is neglected. So if $\ell \approx 2a$ and if N is large then d is large compared to ℓ or $2a$ by a factor of πN . By appropriate use of the distributed signal inputs and shorting conductors one would like to shorten the wavelength associated with the upper frequency response from something of the order of d toward ℓ or $2a$.

The uniform spacing of the signal input positions along the winding length tends to make the loop insensitive to the higher order current modes in the Fourier expansion of the current on the winding "transmission line" for the same reason as with the cylindrical loop in ref. 5. Thus with n signal input positions one would expect to reduce the effects associated with eigenmodes for $n_1 = 1$ through $n_1 = n - 1$. However, since the transmission line model is only very rough one would not expect the higher frequency resonances to be exactly associated with single terms in such a Fourier expansion and the cancellation might not be exact unless some symmetry in the exact winding geometry were being used to cancel the particular resonance. Not only does increasing n make the loop insensitive to some resonances; it also decreases the effective gap capacitance as discussed in ref. 5 by effectively placing n gaps in series. The actual gap impedance effects here are more complex and are important only at rather high frequency compared with some of the resonances on the loop winding; this capacitance benefit is then secondary.

Besides the n signal introduction positions there are n shorting positions as shown in figure 6A for $n = 4$. These shorting positions, if used, alter significantly the resonant mode behavior on the loop winding by raising the first resonant frequencies. To see this result one must shrink the winding from figure 6A to that in figure 6B. The total winding length is d but the shorting conductors have length of the order of a or a little larger including part of the central conductor. The length of a turn group winding is d/n and is typically large compared to a giving the extended winding plus shorting conductor layout shown in figure 6B. Note now that including the shorting conductors in a transmission line model of the winding breaks up the lower order resonances. There can be a resonance for the wavelength of the order of the turn group winding length d/n (or better $2a + d/n$) which is typically small compared to d . There are resonant lengths associated with two turns groups, but no larger since they all come to a common shorting conductor (the central conductor); for such a resonance on two turn groups with shorting conductor bringing the two turn group loop together to form two loops joined at one position, the signal input positions are located for minimum sensitivity to the current in this resonant mode because of the current maximum near the shorting conductor. Thus one would roughly estimate d/n as the longest wavelength associated with a resonant mode on the winding that might couple significantly to the loop output. Of course the resonant modes on the various turn groups couple to

other turn groups through electromagnetic fields and the shared shorted conductors. This complicates the results considerably. However the use of multi-ax winding with shorting conductors attached between the signal input positions does raise the frequencies at which resonances on the loop structure first occur thereby improving the response of the multiturn loop at high frequencies. As a further refinement one might even make the shorting conductors (or some of them) somewhat resistive in an attempt to damp some of the resonances. Hopefully some future notes can consider some boundary value problem solutions pertaining to some multiturn loops at high frequencies to better quantify some of the above considerations.

III. Combining Good Conductors with Imperfectly Conducting Shields

A previous note⁶ has considered the use of one or more conducting shields to improve the performance of electrically small loops. Such a shield has a surface conductance G_s small enough that the magnetic field is negligibly affected by the presence of the shield at frequencies of interest. If the shield cylindrical radius is a_s then we have a characteristic radian frequency for the shield as

$$\omega_s \equiv \frac{2}{\mu_0 a_s G_s} \quad (4)$$

where we have taken the permeability as that of free space. If l_s is the shield length then, of course, we require

$$a_s > a, \quad l_s > l \quad (5)$$

Also make the insulating materials in the loop structure have permittivity not much larger than ϵ_0 and/or occupy a sufficiently small portion of the volume so that wavelengths in the vicinity of the structure are comparable to those outside (taken as free space). Then as long as wavelengths are large compared to both l and $2a_s$ the magnetic field inside the shield is related to the incident magnetic field (taken parallel to the cylinder axis) in the frequency domain as

6. Capt Carl E. Baum, Sensor and Simulation Note 40, Conducting Shields for Electrically-Small Cylindrical Loops, May 1967.

$$\frac{B}{B_{inc}} \approx \left[1 + \frac{i\omega}{\omega_s} \right]^{-1} \quad (6)$$

which assumes $\ell_s \gg a_s$ which is not typically the case where ℓ_s might be roughly $2a_s$. Nevertheless this establishes ω_s as a characteristic frequency for the shield, at least approximately.

The presence of the loop modifies the results of equation 4 somewhat. If the loop has inductance L and drives an output resistive impedance Z_c then we have a characteristic frequency for the loop as

$$\omega_\ell \equiv \frac{Z_c}{L} \quad (7)$$

For radian frequency $\omega > \omega_\ell$ the loop output is proportional to the magnetic field until other high frequency effects set in; for $\omega < \omega_\ell$ the output is proportional to the time rate of change of B or $i\omega B$. Including the presence of the loop one can approximate the loop response function to $i\omega B_{inc}$ as

$$\frac{i\omega B}{i\omega B_{inc}} = \frac{B}{B_{inc}} \approx \left\{ \left[1 + \frac{i\omega}{\omega_\ell} \right] \left[1 + \frac{i\omega}{\omega_s} \right] - \left(\frac{a}{a_s} \right)^2 \frac{i\omega}{\omega_\ell} \frac{i\omega}{\omega_s} \right\}^{-1} \quad (8)$$

where all these results are taken directly from ref. 6. Suppose that we have the inequality $\omega_s \gg \omega_\ell$ so that the loop is well into the integrating mode of operation before the shield starts to exclude magnetic field. Then for all ω with wavelengths large compared to ℓ_s and $2a_s$ we have the approximate result

$$\begin{aligned} \frac{B}{B_{inc}} &\approx \left[1 + \frac{i\omega}{\omega_\ell} \right]^{-1} \left\{ 1 + \frac{i\omega}{\omega_s} \left[1 - \left(\frac{a}{a_s} \right)^2 \left[1 + \frac{\omega_\ell}{i\omega} \right]^{-1} \right] \right\}^{-1} \\ &= \left[1 + \frac{i\omega}{\omega_\ell} \right]^{-1} \left\{ 1 + \frac{i\omega}{\omega_s} \left[1 - \left(\frac{a}{a_s} \right)^2 \right] + \frac{\omega_\ell}{\omega_s} \left(\frac{a}{a_s} \right)^2 \left[1 + \frac{\omega_\ell}{i\omega} \right]^{-1} \right\}^{-1} \\ &\approx \left[1 + \frac{i\omega}{\omega_\ell} \right]^{-1} \left\{ 1 + \frac{i\omega}{\omega_s} \left[1 - \left(\frac{a}{a_s} \right)^2 \right] \right\}^{-1} \quad (9) \end{aligned}$$

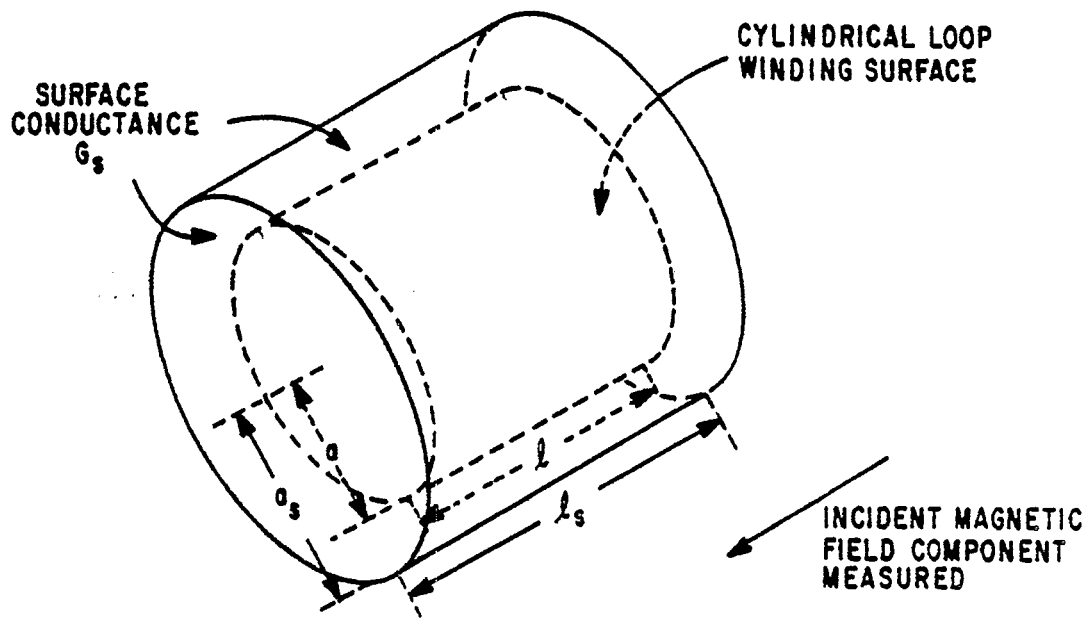
so that for $\omega_s \gg \omega_l$ the factor involving a/a_s effectively raises the characteristic shield frequency from ω_s to ω'_s where

$$\omega'_s \approx \omega_s \left[1 - \left(\frac{a}{a_s} \right)^2 \right]^{-1} \quad (10)$$

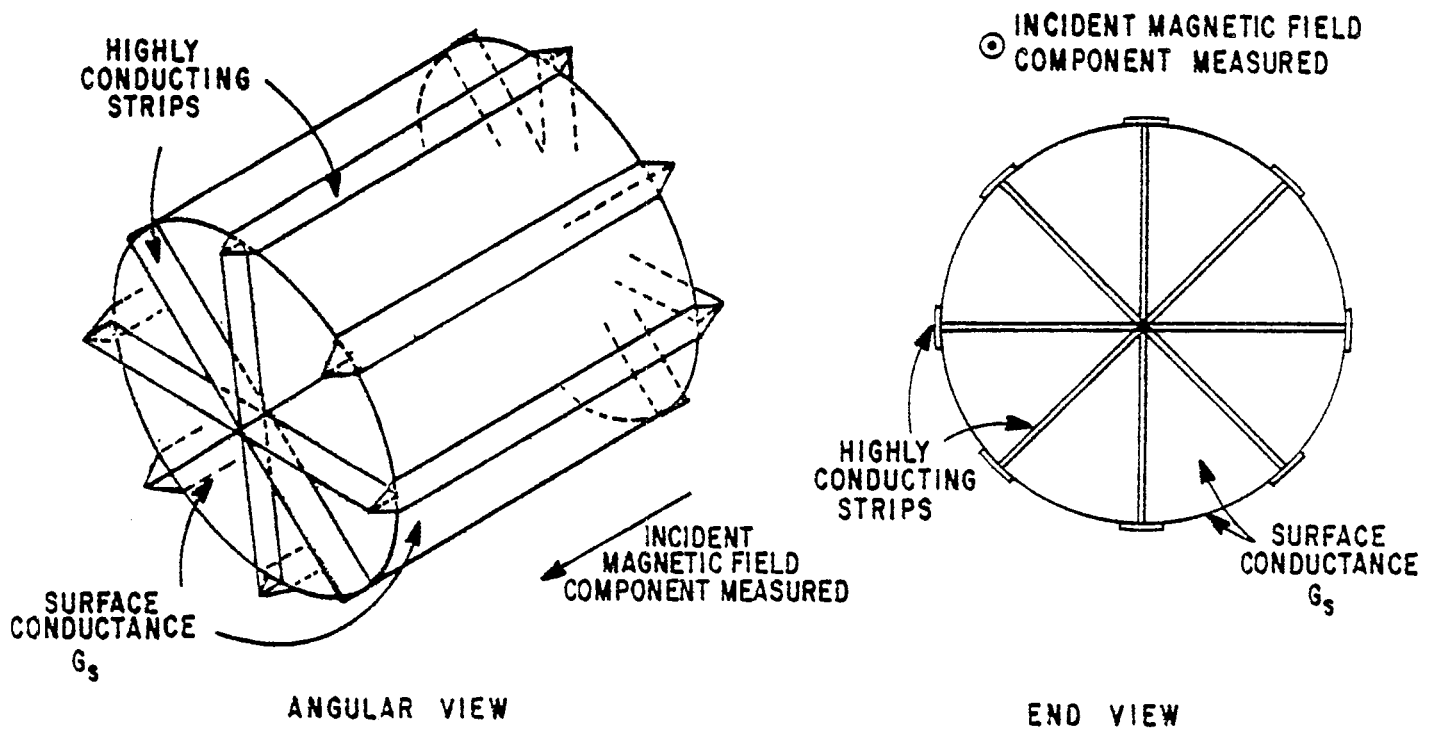
Again since the loop and shield lengths are finite these results are not accurate but give the trend in the response due to the presence of the shield.

Besides reducing unwanted electric field components inside the shield without distorting the magnetic field for ω less than ω_s or ω'_s as appropriate, the shield can serve another helpful role in damping somewhat resonances on the loop structure such as those associated with the winding length for the loop or for turn groups in the loop. Associated with the various resonant modes on the multiturn loop there are current distributions and associated field distributions, both electric and magnetic. The electric field induces a surface current density in the finite non zero surface conductance G_s of the shield thereby extracting energy and damping the mode. How much damping is obtained depends on the details of the winding, its proximity to the shield, and the surface conductance G_s . Perhaps appropriate boundary value problems can be used to quantify this effect and can be discussed in future notes.

The shield geometry we have been considering thus far is shown in figure 7A in which a surface conductance G_s lies on a closed surface (except for signal output) consisting of a finite circular cylinder with flat end caps. The loop winding is contained inside this surface in a symmetrical and coaxial position with respect to the shield. One may have some problems with practical shields of this type related to such things as the uniformity of G_s over the shield surface or breaks in the shield where parts of the shield come together for assembly and disassembly. Such nonuniformities can degrade the axial symmetry of the shield so that an incident magnetic field perpendicular to the cylinder axis can penetrate the shield in a nonsymmetric manner so as to give some coupling to the loop even though it is symmetrically placed inside the shield. At sufficiently low frequencies the magnetic field is negligibly affected by the shield and the problem of shield asymmetry goes away. One might try to avoid such problems by making the shield joints for opening the shield at positions for which a poor joint has minimum tendency to couple unwanted magnetic field components to the loop such as by making breaks along circles in planes perpendicular to the cylinder axis so as to not interfere with azimuthal currents on the shield associated with the axial magnetic field component of interest.



A. SHIELD OF FINITE SURFACE CONDUCTANCE CONTAINING LOOP



B. HIGHLY CONDUCTING CURRENT PATHS ADDED TO SHIELD: EXAMPLE WITH EIGHT AXIAL PATHS

FIGURE 7. SHIELD USED WITH A CYLINDRICAL LOOP

Recognizing that it is only the azimuthal currents on the shield which are associated with the axially symmetric part of the magnetic field distribution of interest then the shield need only allow in an axial magnetic field by presenting a resistive path to the azimuthal surface current density. The radial surface currents on the end caps and the axial surface currents on the finite circular cylinder portion of the shield might just as well flow through infinite surface conductance (zero surface resistance). This would have the advantage of significantly reducing the penetration of incident magnetic field components perpendicular to the loop axis into the shield volume to interact with the loop structure. Such a shield structure would be characterized by an anisotropic surface conductance. It would be very highly conducting in one direction but only moderately conducting in the other direction with value G_s related to the desired ω_s as in equation 4. One might call this kind of a shield an anisotropic conducting shield.

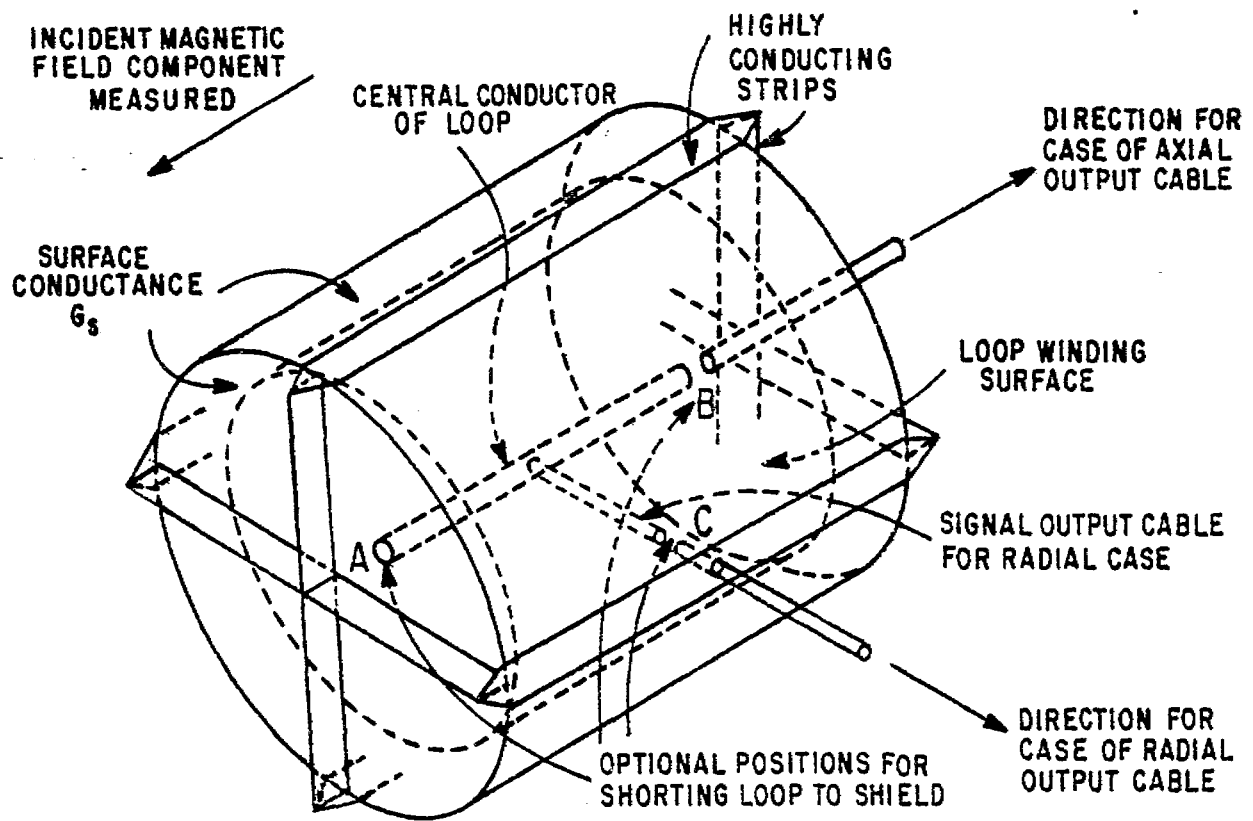
One configuration for a realization of such an anisotropic shield is shown in figure 7B. In this example there are a number of highly conducting strips running axially evenly spaced around the cylindrical portion of the shield surface; on the end caps highly conducting radial strips are used to connect each axial strip to two common tie points on the sensor and shield axis. As shown in the end view in figure 7B the strips are aligned so as to present negligible cross section to an axial magnetic field, the field component of interest. Thus while the axial strips can lie on the cylindrical portion of the shield as part of that surface, the radial strips on the end caps lie in planes through the shield axis and thus perpendicular to the end caps. While the strips on the cylindrical part of the shield do carry azimuthal currents across their width this is not a serious problem because the finitely conducting material between the strips still presents an impedance to the azimuthal surface current so that if one wishes G_s can be lowered to compensate for the fraction of the azimuthal path around the cylindrical part of the shield surface which is occupied by the axial conducting strips. If the shield is broken for entry along an azimuthal path then the conducting strips can end in highly conducting contact positions along the break path; these contact positions can be used to reestablish the highly conducting paths between the shield parts when they are rejoined.

These shorting turns around the shield surface have other effects besides reducing the magnetic field components perpendicular to the sensor axis. The shorting conductors quickly redistribute current over the shield surface along paths which give negligible coupling of the currents to the loop inside which is ideally axially symmetric. One example of such currents would be those flowing onto the shield from the outer conductor of a signal cable which is designed to transport the sensor signal to some other location. The outer conductor of this cable must be attached to the sensor shield where it penetrates

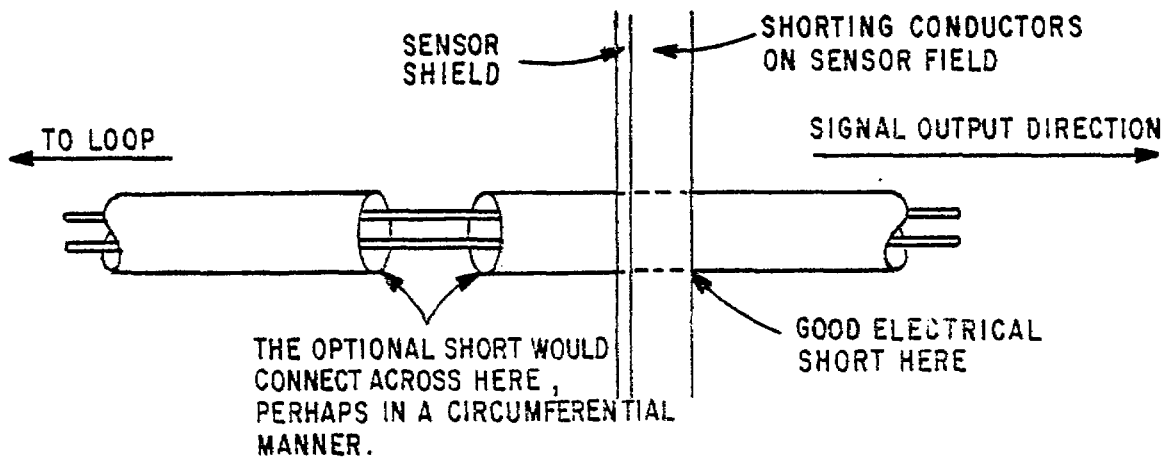
the shield if the sensor shield is to divert the currents flowing on the outside of the signal cable away from the sensor to the shield. In penetrating the sensor shield the cable should then do it at a place where there is one or more of the shorting conductors on the shield. For the axial signal output configuration as in figure 2A the signal output cable is on the sensor and shield axis and thus conveniently passes through the junction of the radial shorting strips on one of the shield end caps. For the radial signal output configuration as in figure 2B the signal cable can easily be made to intersect with one of the axial shorting strips on the cylindrical portion of the sensor shield simply by appropriately rotating the sensor shield with respect to the sensor and the signal output cable. The shorting strips on the shield also have some effect on the damping of resonances on the loop structure if any axial and/or radial currents are induced on the shield associated with the resonances since axial and radial currents can flow on paths of high conductance. One may then wish to adjust G_s for the moderately conducting part of the shield to compensate for the presence of the shorting strips and more optimally damp the resonances on the loop structure which have the greatest effect on the signal output from the sensor.

Having considered the finitely conducting shield combined with radial and axial highly conducting current paths let us now consider some features of the connection of the differential signal output cable to the sensor. As the signal output cable reaches the sensor by passing through the sensor shield its outer conductor is electrically connected to the sensor shield at the penetration position which is chosen where there is one or more of the highly conducting current paths on the sensor shield. Figure 2 shows the geometry of the signal output cable with respect to the sensor for both axial and radial signal output configurations. Figure 8A shows 3 points of interest on the sensor shield that apply to one or both of these output configurations. Two of these positions (labelled A and B) are on the shield axis on the two end caps where contact can be made with all the radial shorting conductors; the third position (labelled C) is on the cylindrical portion of the shield midway between the two end caps and in the center of one of the axial shorting conductors.

On penetrating the shield, say at points B or C, the signal mode of the differential signal output cable must connect into the sensor. This signal output cable might be twinax or two coaxes with outer conductors electrically bonded together to operate as a twinax. Note that there is no fundamental necessity for the output cable to have its outer conductor continuous so as to electrically connect the shield to the sensor structure. The differential mode of signal propagation on a twinax has no net current on the cable shield associated with it. As shown in figure 8B the twinax (or dual coax) shield can be broken or even provided with an optional electrical connection



A. GEOMETRY OF SOME OPTIONAL SHORTING POSITIONS BETWEEN THE LOOP AND THE SENSOR SHIELD : EXAMPLE WITH FOUR AXIAL SHORTING PATHS



B. OPTIONAL ELECTRICAL SHORT AT BREAK IN TWINAX OUTPUT CABLE SHIELD

FIGURE 8. SIGNAL OUTPUT CONNECTION THROUGH THE SENSOR SHIELD

which can be opened or closed as desired. If the section of cable shield removed is short only a very small perturbation applying to correspondingly high frequencies is introduced into the differential mode signal. Thus one can build such a shielded multiturn loop with the loop either electrically floating with respect to the twinax shield of the output or electrically shorted to it, or even connected to it through some other impedance. If the loop is shorted to the output cable shield and thus to the sensor shield at the position where the output cable penetrates the sensor shield, then one may wish to short the loop structure to the sensor shield at other convenient positions to allow the current to redistribute even more rapidly (giving an effectively smaller inductance to the electrical connection). Consider the case of axial signal output from position B. One might conveniently use position A for a shorting connection between the radial conductors on this end cap to the central conductor in the loop structure. Position C would not be used for this case unless one wished to connect from here (as well as other axial shorting conductors on the shield) via a radial path to the loop central conductor. Next consider the case of radial signal output from position C. For this case shorting connections from both end caps to the loop central conductor could appropriately be made at positions A and B.

It is normally very desirable to have the output cable shield connect to the sensor shield so that large currents induced on the cable outer conductor by the external fields can flow onto the sensor shield and not couple significantly through the electrostatic shield to the sensor producing a large common mode signal in the twinax. For the same reason if there were no sensor shield the loop structure including the multi-ax winding shield would be connected to the output cable shield. Other factors, however, can enter the picture. If the cable shield of the signal output cable is not sufficiently highly conducting the currents induced on this cable shield by the external fields can couple into the interior of the cable and give a significant common mode signal. For low frequency operation of the sensor one might then have the sensor floating with respect to this cable shield so that there is a large common mode impedance at the sensor end of the cable, thereby reducing the common mode signal at the other end. On the other hand one may have some undesirable common mode resonances in the sensor-shield structure and/or output cable that might be bothersome for a floating loop structure. If nuclear radiation is present during the magnetic field measurement to a significant degree then one would strongly prefer to short out the common mode radiation signal at the sensor to minimize the amount being transported to the load via the output cable. This would favor the shorting of the loop structure to the sensor shield via the output cable shield and other shorting positions mentioned above. For use in nuclear radiation environments this shorting technique is one form of the "center point grounding" technique mentioned in section II. Of course if the signal output cable is adequately

shielded there is no big reason not to have the loop structure shorted to the sensor shield.

IV. Loop Inductance for Uniformly Spaced Turns

If the cylindrical loop of length l and radius a is assumed to have a uniform turns density along its length then one can approximate this winding by a uniform azimuthal surface current density. The inductance of the loop for such a case has been considered in a previous note (ref. 3) and can be expressed as

$$L = N^2 \mu_0 \frac{\pi a^2}{l} f(\xi) \quad (11)$$

$$f(\xi) = \frac{4}{3\pi\xi} \left[(1 + \xi^2)^{1/2} (1 - \xi^2) E(m) + \xi^2 (1 + \xi^2)^{1/2} K(m) - 1 \right]$$

where $f(\xi)$ is a dimensionless factor in the inductance which gives a correction factor to multiply by the infinite solenoid approximation to obtain the accurate inductance of the finite uniform cylindrical current sheet. The dimensions l and a enter into the factor

$$\xi \equiv \frac{l}{2a} \quad (12)$$

which is simply the length to diameter ratio and the complete elliptic integrals K and E are functions of what is called the parameter m where

$$m \equiv 1 - m_1 = [1 + \xi^2]^{-1} \quad (13)$$

with m_1 called the complementary parameter.

For large ξ the dimensionless factor can be expanded for $m \rightarrow 0$ and $\xi \rightarrow \infty$ as

$$\begin{aligned}
f(\xi) &= \frac{4}{3\pi\xi} \left[\frac{3\pi}{4} m^{-1/2} - 1 + O(m^{1/2}) \right] \\
&= 1 - \frac{4}{3\pi\xi} + O(\xi^{-2})
\end{aligned} \tag{14}$$

For small ξ with $\xi \rightarrow 0$ and $m_1 \rightarrow 0$ we have

$$\begin{aligned}
f(\xi) &= \frac{\sqrt{m_1}}{\pi} \left[\ln\left(\frac{16}{m_1}\right) - 1 \right] [1 + O(m_1)] \\
&= \frac{2\xi}{\pi} \left[\ln\left(\frac{4}{\xi}\right) - \frac{1}{2} \right] [1 + O(\xi^2)]
\end{aligned} \tag{15}$$

For reference $f(\xi)$ is tabulated in tables 1A and 1B for $.1 < \xi < 70$ and is compared for small ξ with the asymptotic form in equation 15 and for large ξ with that in equation 14. For $\xi = .1$ the relative difference is about 10^{-3} and for $\xi = 70$ the relative difference is about 10^{-4} so that the asymptotic forms can be used quite accurately outside the range of the tables. This function $f(\xi)$ is related to the inductance functions tabulated in another reference.⁷

The inductance of a multiturn cylindrical loop with N uniformly spaced turns is of course not quite the same as that calculated using a uniform azimuthal surface current density on the cylindrical winding surface of length l and radius a . If the surface current density is oriented as in figure 9A the magnetic fields on the two sides are related through

$$(\vec{H}_1 - \vec{H}_2) \times \vec{e}_y = \vec{J}_s \tag{16}$$

where we have local cartesian coordinates as shown and \vec{e}_y is a unit vector in the y direction (perpendicular to the current sheet). Here we have approximated the loop winding surface as a plane which applies to our present calculations as long as $p \ll a$ where $2p$ is the spacing between turns which is related to the number of turns N and length of the winding surface as

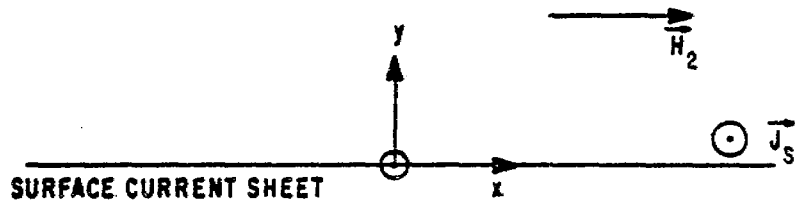
7. E. Jahnke and F. Emde, Tables of Functions with Formulas and Curves, 4th ed., Dover, 1945, pp. 88, 89.

ξ	$f(\xi)$	$\frac{2\xi}{\pi} \left[\ln\left(\frac{4}{\xi}\right) - \frac{1}{2} \right]$	ξ	$f(\xi)$
.100	.2033	.2030	.500	.5255
.105	.2103	.2099	.525	.5373
.110	.2170	.2166	.550	.5486
.115	.2237	.2232	.575	.5594
.120	.2302	.2297	.600	.5697
.125	.2366	.2360	.625	.5795
.130	.2428	.2422	.650	.5890
.135	.2490	.2483	.675	.5980
.140	.2550	.2542	.700	.6067
.145	.2609	.2601	.725	.6150
.150	.2667	.2658	.750	.6230
.155	.2725	.2714	.775	.6307
.160	.2781	.2769	.800	.6381
.165	.2836	.2824	.825	.6452
.170	.2890	.2877	.850	.6521
.175	.2944	.2929	.875	.6587
.180	.2996	.2981	.900	.6651
.185	.3048	.3031	.925	.6712
.190	.3099	.3081	.950	.6771
.195	.3149	.3130	.975	.6829
.200	.3198	.3178	1.000	.6884
.210	.3295	.3271	1.050	.6990
.220	.3389	.3362	1.100	.7089
.230	.3480	.3450	1.150	.7181
.240	.3568	.3535	1.200	.7269
.250	.3654	.3617	1.250	.7351
.260	.3738	.3697	1.300	.7428
.270	.3820	.3774	1.350	.7502
.280	.3899	.3849	1.400	.7571
.290	.3977	.3922	1.450	.7637
.300	.4053	.3992	1.500	.7699
.310	.4127	.4060	1.550	.7758
.320	.4199	.4127	1.600	.7814
.330	.4269	.4191	1.650	.7868
.340	.4338	.4253	1.700	.7919
.350	.4405	.4314	1.750	.7968
.360	.4470	.4373	1.800	.8014
.370	.4535	.4430	1.850	.8059
.380	.4597	.4485	1.900	.8101
.390	.4659	.4538	1.950	.8142
.400	.4719	.4590	2.000	.8181
.410	.4777	.4641	2.100	.8255
.420	.4835	.4689	2.200	.8323
.430	.4891	.4737	2.300	.8386
.440	.4946	.4782	2.400	.8444
.450	.5001	.4827	2.500	.8499
.460	.5053	.4869	2.600	.8549
.470	.5105	.4911	2.700	.8597
.480	.5156	.4951	2.800	.8641
.490	.5206	.4990	2.900	.8683

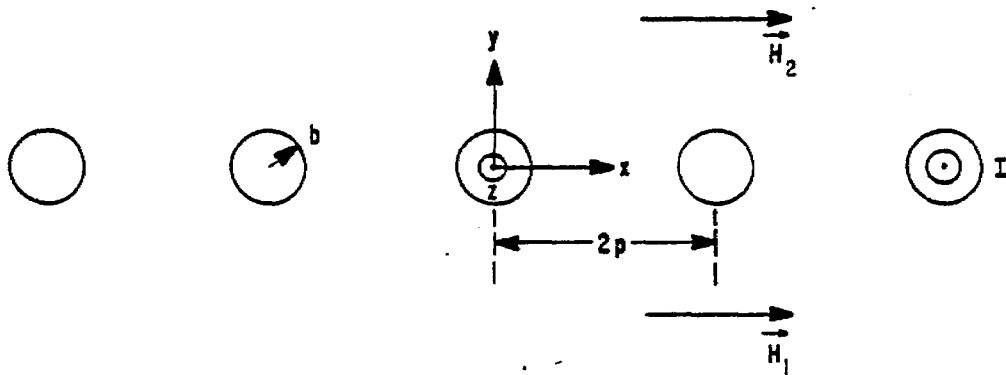
Table 1A. Dimensionless factor in loop inductance for small arguments

ξ	$f(\xi)$	$1 - \frac{4}{3\pi\xi}$	ξ	$f(\xi)$	$1 - \frac{4}{3\pi\xi}$
3.00	.8722	.8585	15.0	.9723	.9717
3.10	.8759	.8631	15.5	.9731	.9726
3.20	.8794	.8674	16.0	.9740	.9735
3.30	.8827	.8714	16.5	.9747	.9743
3.40	.8859	.8752	17.0	.9755	.9750
3.50	.8888	.8787	17.5	.9762	.9757
3.60	.8917	.8821	18.0	.9768	.9764
3.70	.8943	.8853	18.5	.9774	.9771
3.80	.8969	.8883	19.0	.9780	.9777
3.90	.8993	.8912	19.5	.9786	.9782
4.00	.9016	.8939	20.0	.9791	.9788
4.10	.9039	.8965	21.0	.9801	.9798
4.20	.9060	.8989	22.0	.9810	.9807
4.30	.9080	.9013	23.0	.9818	.9815
4.40	.9100	.9035	24.0	.9825	.9823
4.50	.9118	.9057	25.0	.9832	.9830
4.60	.9136	.9077	26.0	.9839	.9837
4.70	.9153	.9097	27.0	.9845	.9843
4.80	.9170	.9116	28.0	.9850	.9848
4.90	.9186	.9134	29.0	.9855	.9854
5.00	.9201	.9151	30.0	.9860	.9859
5.25	.9237	.9192	31.0	.9864	.9863
5.50	.9269	.9228	32.0	.9869	.9867
5.75	.9300	.9262	33.0	.9873	.9871
6.00	.9327	.9293	34.0	.9876	.9875
6.25	.9353	.9321	35.0	.9880	.9879
6.50	.9377	.9347	36.0	.9883	.9882
6.75	.9399	.9371	37.0	.9886	.9885
7.00	.9419	.9394	38.0	.9889	.9888
7.25	.9438	.9415	39.0	.9892	.9891
7.50	.9456	.9434	40.0	.9895	.9894
7.75	.9473	.9452	41.0	.9897	.9896
8.00	.9489	.9469	42.0	.9900	.9899
8.25	.9504	.9486	43.0	.9902	.9901
8.50	.9518	.9501	44.0	.9904	.9904
8.75	.9531	.9515	45.0	.9906	.9906
9.00	.9544	.9528	46.0	.9908	.9908
9.25	.9556	.9541	47.0	.9910	.9910
9.50	.9567	.9553	48.0	.9912	.9912
9.75	.9578	.9565	49.0	.9914	.9913
10.00	.9588	.9576	50.0	.9916	.9915
10.50	.9607	.9596	52.5	.9920	.9919
11.00	.9624	.9614	55.0	.9923	.9923
11.50	.9640	.9631	57.5	.9927	.9926
12.00	.9655	.9646	60.0	.9930	.9929
12.50	.9668	.9660	62.5	.9932	.9932
13.00	.9681	.9674	65.0	.9935	.9935
13.50	.9692	.9686	67.5	.9937	.9937
14.00	.9703	.9697	70.0	.9940	.9939
14.50	.9713	.9707			

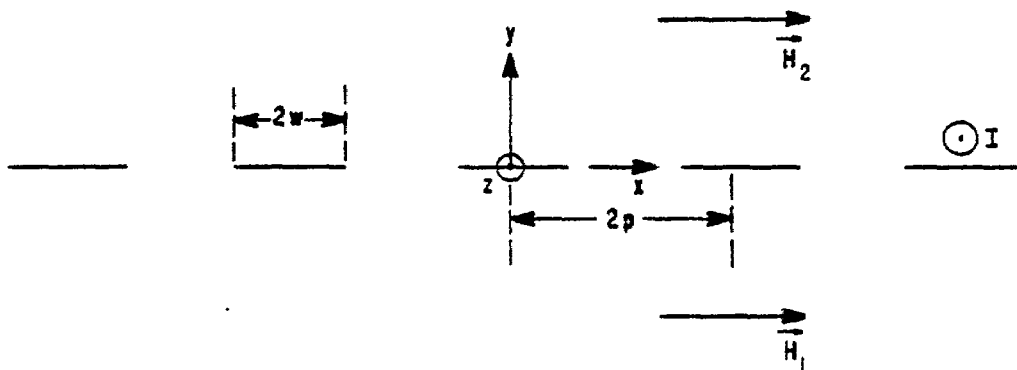
Table 1B. Dimensionless factor in loop inductance for large arguments



A. UNIFORM SURFACE CURRENT DENSITY WITH MAGNETIC FIELDS PARALLEL TO THE SURFACE AND PERPENDICULAR TO \vec{J}_s



B. UNIFORMLY SPACED CIRCULAR WIRES WITH LOCAL COORDINATES



C. UNIFORMLY SPACED FLAT STRIPS WITH LOCAL COORDINATES

FIGURE 9. APPROXIMATION OF UNIFORMLY SPACED LOOP TURNS BY A UNIFORM CURRENT SHEET

$$p = \frac{\ell}{2N} \quad (17)$$

assuming a uniform winding spacing and all loop turns electrically in series.

Figure 9 shows two types of windings. Figure 9B shows circular wires of radius b which we take to be perfectly conducting. This case applies to the multi-ax winding discussed in section 2 as well as to plain circular wire. Figure 9C shows thin flat strips which we take to be perfectly conducting. These are not all the cases one might imagine but they do apply to the most common situations.

Note for these calculations we take \vec{H}_1 and \vec{H}_2 as having only x components. Because of the approximate axial symmetry of the loop winding the z component can be neglected for these calculations. However the magnetic field produced by the loop current will in general have a y component because of the finite length ℓ . While the loop winding can distort this y component as it passes through the winding surface we do not consider this effect here. Near the lengthwise center of the winding surface this component is zero by symmetry. However near the ends of the winding surface it is significant. Thus let us consider H_1 and H_2 to be the scalar x components and J_s to be the z component of the surface current density which we relate to the current I carried by each loop turn as

$$I = 2pJ_s \quad (18)$$

What we wish to calculate is the extra inductance associated with confining the current to the surface of wire or strip conductors.

For the case of circular wires in figure 9B we can use some results from a previous note if the wires are small.⁸ Suppose the side with H_1 is the interior of the loop volume. Then we wish to calculate the additional flux per unit wire length on this side of the wire. From reference 8 we have an effective displacement to an equivalent uniform plane from the grid as

$$\Delta_1 \approx \frac{p}{\pi} \ln\left(\frac{p}{\pi b}\right) \quad (19)$$

8. Lt Carl E. Baum, Sensor and Simulation Note 21, Impedances and Field Distributions for Parallel Plate Transmission Line Simulators, June 1966.

and if we take another case that $H_2 = -H_1$ to give opposite magnetic fields on the two sides we have an effective displacement

$$\Delta_2 \approx \frac{2p}{\pi} \ln\left(\frac{p}{\pi b}\right) \quad (20)$$

These Δ s are basically obtained by dividing the extra flux per unit wire length on one side of the wire, say for $y < -b$ along $x = 0$, by the distant magnetic field on that side. These same results apply to capacitance calculations and transmission line impedance calculations because we are using a two dimensional approximation with everything assumed independent of z .

For a current I the extra magnetic flux per unit wire length is then, using equation 19,

$$\Delta\phi = \mu_0 H_1 \Delta_1 = \mu_0 \frac{I}{2p} \Delta_1 \quad (21)$$

since for this case

$$H_1 = \frac{I}{2p} \quad (22)$$

For the case with equal but opposite magnetic fields on opposite sides of the winding we have

$$\Delta\phi = \mu_0 H_1 \Delta_2 = \mu_0 \frac{I}{4p} \Delta_2 \quad (23)$$

since for this case

$$H_1 = \frac{I}{4p} \quad (24)$$

or half as much as in the first case. Note that equations 21 and 23 give the same results as

$$\Delta\phi \approx \frac{\mu_0}{2\pi} I \ln\left(\frac{p}{\pi b}\right) \quad (25)$$

It is only the difference between H_1 and H_2 that enters into the calculation as long as the wire thickness in the y direction is negligibly small so that a uniform magnetic field in the x direction is not significantly pushed away from the wire grid with zero net current by the wire thickness.

Having the extra flux per unit wire length then the extra flux per turn is

$$2\pi a \Delta \phi = \mu_0 \frac{\pi a}{2p} \Delta_2 I \approx \mu_0 a \ln\left(\frac{p}{\pi b}\right) I \quad (26)$$

For a uniform loop winding of N series turns the added inductance is then

$$\Delta L = \frac{N^2 \pi a \Delta \phi}{I} = N \mu_0 \frac{\pi a}{2p} \Delta_2 \approx N \mu_0 a \ln\left(\frac{p}{\pi b}\right) \quad (27)$$

For a nonuniformly spaced loop winding one could sum the contributions associated with each turn instead of simply multiplying by N.

The result of equation 27 is based on a small wire size (or multi-ax outer shield size) such that $b \ll p$. If the wire size gets large so that $b < p$ but not greatly so one can use the results in another more recent note.⁹ Here exact solutions are obtained for fat rods. In figure 27 of that note δ_1 , δ_2 , and δ_3 are plotted as functions of what is b/p in our notation in this note. The δ s are related to

$$\Delta_1 \equiv p \delta_1, \quad \Delta_2 \equiv p \delta_2, \quad \Delta_3 \equiv p \delta_3 \quad (28)$$

where Δ_1 and Δ_2 are what we have listed above in equations 19 and 20 for small b/p . The third one is Δ_3 which corresponds to the case of $H_1 = +H_2$ in figure 9B and is significant when compared to Δ_1 and Δ_2 for fat wires. Using these more accurate results we have for case 1 ($H_2 = 0$)

$$\Delta L = N \mu_0 \frac{\pi a}{p} \Delta_1 = N \mu_0 \pi a \delta_1 \quad (29)$$

9. Lennart Marin, Sensor and Simulation Note 118, Effect of Replacing One Conducting Plate of a Parallel-Plate Transmission Line by a Grid of Rods, October 1970.

and for case 2 ($H_1 = -H_2$)

$$\Delta L = N\mu_0 \frac{\pi a}{p} \frac{\Delta_2}{2} = N\mu_0 \pi a \frac{\delta_2}{2} \quad (30)$$

However, for fat wires $\Delta_1 \neq \Delta_2/2$. With the results for fat wires (applying to fat multiwire) one can find values of b/p to make $\Delta L \approx 0$ if one wishes. For case 1 using small δ_1 we have $\delta_1 = 0$ for $b/p \approx .267$ and similarly for case 2 we have $\delta_2 = 0$ for $b/p \approx .317$. The results for the two cases are not the same but do show that for $b/p \approx .3$ the extra inductance associated with the wires instead of a current sheet goes away but that the best value to use depends on the relative values of H_1 and H_2 .

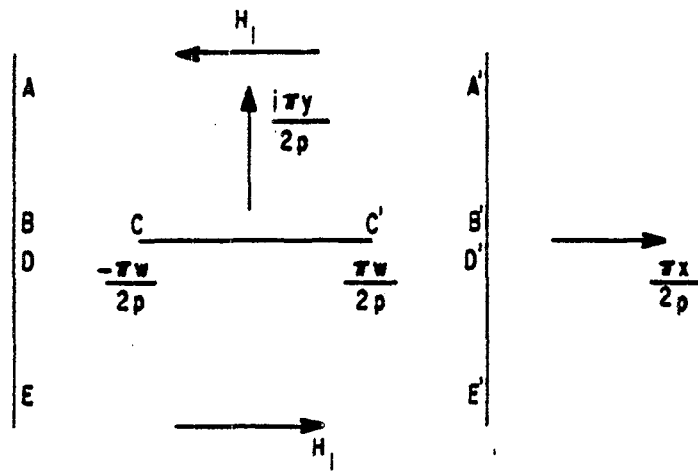
Now we consider the case of a loop winding made of highly conducting strips of width $2w$ as shown in figure 9C. Define complex variables

$$\zeta \equiv \frac{\pi}{2p}[x + iy], \quad \gamma' \equiv \alpha' + i\beta', \quad \gamma \equiv \alpha + i\beta \quad (31)$$

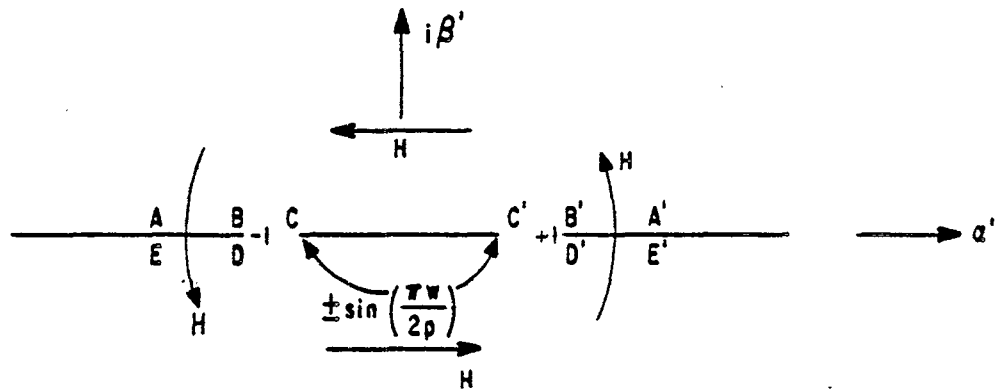
where x and y are the coordinates as shown in figure 9C. We now make a few conformal transformations to obtain the potential and field distributions appropriate to the two dimensional geometry of periodic perfectly conducting strips as shown in figure 9C. One cell in the periodic array of strips has width $2p$ and contains a strip of width $2w$ centered in the cell. In the ζ plane as shown in figure 10A this cell is the range $-\pi/2 < \pi x/(2p) < \pi/2$ with the conducting strip lying on $\pi y/(2p) = 0$ in the range $-\pi w/(2p) < \pi x/(2p) < \pi w/(2p)$. This is mapped onto the γ' plane in figure 10B by the transformation

$$\gamma' = \sin(\zeta), \quad \zeta = \arcsin(\gamma') \quad (32)$$

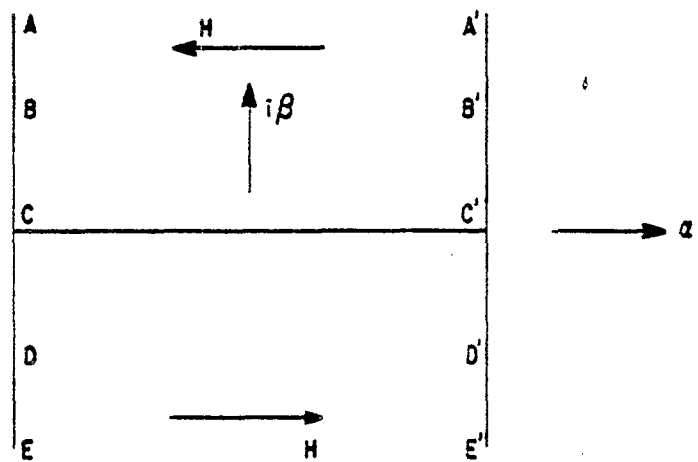
Note how the boundaries in the ζ plane map into those in the γ' plane such that the normal magnetic field is made continuous for $|\alpha'| > \sin(\pi w/(2p))$ through $\beta' = 0$ so that we have one strip in the γ' plane of width $2 \sin(\pi w/(2p))$. A few points on the boundaries in the ζ plane are labelled so that one can see how they transform into the γ' plane and then into the γ plane in figure 10C via the transformation



A. ζ PLANE



B. γ' PLANE



C. γ PLANE

FIGURE 10. CONFORMAL TRANSFORMATIONS FOR CASE OF PERIODIC THIN PERFECTLY CONDUCTING STRIPS

$$\gamma = \arcsin \left[\frac{\gamma'}{\sin\left(\frac{\pi w}{2p}\right)} \right] = \arcsin \left[\frac{\sin(\zeta)}{\sin\left(\frac{\pi w}{2p}\right)} \right] \quad (33)$$

$$\zeta = \arcsin \left[\sin\left(\frac{\pi w}{2p}\right) \sin(\gamma) \right]$$

In figure 10C we have boundaries at $\alpha = +\pi/2$ and at $\beta = 0$. For $\beta > 0$ the magnetic field has a direction everywhere parallel to the α axis and is uniform, while for $\beta < 0$ the magnetic field has the opposite direction but is still uniform.

From equations 33 one can plot contours of constant α and constant β in the ζ plane to give equipotential lines for these two potential functions. Referring to figure 10C the potential function of interest we use is β . Along the contour $\alpha = 0$ we also have $\text{Re}[\zeta] = 0$ in the ζ plane. The magnetic flux between the conducting strip (CC') and some other position is proportional to β and the magnetic field is proportional to the gradient of β but at a right angle to it. For convenience along $x = 0$ with $y > 0$ then using our two dimensional model we evaluate the effective shift of the conducting strips to an equivalent conducting plane as

$$\Delta_2 = \lim_{y \rightarrow \infty} \frac{\beta}{\frac{\partial \beta}{\partial y} \Big|_{y=\infty}} - y \quad (34)$$

On $x = 0$ we have

$$\alpha = 0$$

$$\beta = \text{arcsinh} \left[\frac{\sinh \frac{\pi y}{2p}}{\sin \frac{\pi w}{2p}} \right] \quad (35)$$

For large y on $x = 0$ we have

$$\begin{aligned}
\beta &= \ln \left[\frac{e^{\frac{\pi y}{2p}} - e^{-\frac{\pi y}{2p}}}{2 \sin\left(\frac{\pi w}{2p}\right)} + \left(\frac{e^{\frac{\pi y}{p}} + e^{-\frac{\pi y}{p}} - 2}{4 \sin^2\left(\frac{\pi w}{2p}\right)} + 1 \right)^{1/2} \right] \\
&= \frac{\pi y}{2p} - \ln \left[\sin\left(\frac{\pi w}{2p}\right) \right] + \ln \left[\frac{1}{2} \left[1 - e^{-\frac{\pi y}{p}} + \left(1 + e^{-\frac{2\pi y}{p}} \right. \right. \right. \\
&\quad \left. \left. \left. + \left[4 \sin^2\left(\frac{\pi w}{2p}\right) - 2 \right] e^{-\frac{\pi y}{p}} \right)^{1/2} \right] \right] \\
&= \frac{\pi y}{2p} - \ln \left[\sin\left(\frac{\pi w}{2p}\right) \right] + \ln \left[1 + o\left(e^{-\frac{\pi y}{p}}\right) \right] \\
&= \frac{\pi y}{2p} - \ln \left[\sin\left(\frac{\pi w}{2p}\right) \right] + o\left(e^{-\frac{\pi y}{p}}\right) \tag{36}
\end{aligned}$$

giving for Δ_2 the result

$$\Delta_2 = -\frac{2p}{\pi} \ln \left[\sin\left(\frac{\pi w}{2p}\right) \right] = \frac{2p}{\pi} \ln \left[\csc\left(\frac{\pi w}{2p}\right) \right] \tag{37}$$

From equation 27 the inductance correction for uniformly spaced strips is then

$$\Delta L = N\mu_0 \frac{\pi a}{2p} \Delta_2 = N\mu_0 a \ln \left[\csc\left(\frac{\pi w}{2p}\right) \right] \tag{38}$$

Note that $\Delta L \geq 0$ for $0 < w < p$.

For small w/p we have the asymptotic form for Δ_2 as $w/p \rightarrow 0+$ as

$$\begin{aligned}
\Delta_2 &= -\frac{2p}{\pi} \ln \left[\frac{\pi}{2} \frac{w}{p} \left(1 + o \left(\left(\frac{w}{p} \right)^2 \right) \right) \right] \\
&= \frac{2p}{\pi} \left[\ln \left(\frac{2p}{\pi w} \right) + o \left(\left(\frac{w}{p} \right)^2 \right) \right]
\end{aligned} \tag{39}$$

which can be compared to the result in equation 20 for circular wires. For wide strips with narrow spacing between strips we have the result for $1 - w/p \rightarrow 0+$ as

$$\begin{aligned}
\Delta_2 &= -\frac{2p}{\pi} \ln \left[\cos \left(\frac{\pi}{2} \left(1 - \frac{w}{p} \right) \right) \right] \\
&= -\frac{2p}{\pi} \ln \left[1 - \frac{1}{2} \left(\frac{\pi}{2} \left(1 - \frac{w}{p} \right) \right)^2 + o \left(\left(1 - \frac{w}{p} \right)^4 \right) \right] \\
&= \frac{\pi p}{4} \left[\left(1 - \frac{w}{p} \right)^2 + o \left(\left(1 - \frac{w}{p} \right)^4 \right) \right]
\end{aligned} \tag{40}$$

One obtains the effective displacement for a uniform magnetic field on only one side of the array of conducting strips through the relation

$$\Delta_1 = \frac{\Delta_2}{2} = \frac{p}{\pi} \ln \left[\csc \left(\frac{\pi w}{2p} \right) \right] \tag{41}$$

This factor of 2 relation is exact for the strips (in contrast to the circular wire case) because the perfectly conducting periodic array of flat strips has no thickness perpendicular to the array (i.e. in the y direction). A uniform magnetic field parallel to the strip array can be added equally for both positive and negative y without any associated magnetic field distortion near the strips.

V. Summary

In this note we have considered several aspects of the design of multiturn loops for measuring magnetic fields including some techniques for improving the performance of such sensors. First discussed was an application of multi-ax cable as the loop winding to increase the number of series signal introduction positions from the external electromagnetic fields to the

eventual sensor output. Using this multi-ax technique together with appropriate shorting conductors can add various symmetries to the loop design and break up some of the first resonances (as one goes higher in frequency) of the current on the multi-turn loop winding. There is some asymmetry in the way the turns cross over one another in a counterwound loop design, but the effects of this can be minimized by an appropriate alternation in the crossing sequence. The path of the signal output cable can also be positioned in a few different configurations which minimize the coupling of currents on the outside of this cable to the loop winding.

One interesting technique for use with multiturn loops involves surrounding the loop structure with a finitely conducting shield. This keeps out the incident low frequency electric field but the surface conductance should not be made too large if one wishes to not significantly exclude the incident magnetic field at the high frequencies of interest. Another use for this conducting shield is for introducing damping into resonant current modes on the loop structure by means of the coupling of the associated fields back to the lossy shield. One can modify the shield design by adding good conductors along paths in planes which contain the loop axis and which lie along the surface of the shield; such paths are radial and axial, but not azimuthal. Such highly conducting paths might be made from metal strips. These conducting paths have the effect of excluding incident magnetic field components which are perpendicular to the loop axis. These paths also help to more rapidly redistribute charge and current on the shield surface along paths which ideally have no coupling to the loop winding. In designing such a finitely conducting shield, perhaps with the highly conducting paths, one should be careful to preserve appropriate symmetry of the shield with respect to the loop so that off axis magnetic field components do not couple to the loop to any noticeable degree for frequencies of interest.

One of the important parameters in the loop design is its inductance. For convenience we have tabulated the factor which when multiplied by the simple infinite uniform cylindrical current sheet formula gives the inductance of a finite cylindrical current sheet of arbitrary length to diameter ratio. Real multiturn loops do not have uniform azimuthal surface current densities so we have developed a few correction factors to correct the inductance for the confinement of the current to the surfaces of azimuthal wires (including multi-ax cables) and flat strips.

We would like to thank Mr. Terry L. Brown of Dikewood for the computer calculations and tabulation.